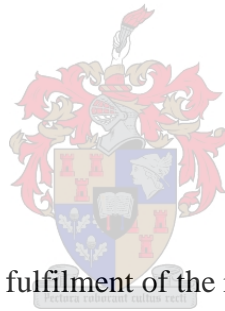


**Non-destructive measurement of citrus internal quality using Near Infrared
Spectroscopy and X-ray Computed Tomography**

by

Phalane Sekina Lebotsa



Thesis presented in partial fulfilment of the requirements for the degree

Master of Science in Engineering at

Stellenbosch University

Supervisors: Prof. U. L Opara, Prof. W. J Perold, Dr H. H Nieuwoudt

March 2017

Declaration

By submitting this thesis electronically, I declare that the entirety of the work contained therein is my own, original work, that I am the sole author thereof (save to the extent explicitly otherwise stated), that reproduction and publication thereof by Stellenbosch University will not infringe any third party rights and that I have not previously in its entirety or in part submitted it for obtaining any qualification.

Date: March 2017

Copyright © 2017 Stellenbosch University

All rights reserved.

Abstract

Quality evaluation of fruit remains an important aspect in the fruit industry. It is for this reason that non-destructive methods for quality evaluation of citrus fruit were investigated. Literature reviews revealed the possibilities of near infrared (NIR) spectroscopy to detect physicochemical properties and X-ray computed tomography (X-ray CT) to investigate internal structure of citrus fruit. The non-destructive methods were also used to classify the citrus fruit based on the quality parameters. First, Fourier transform near infrared (FT-NIR) spectroscopy was used to detect the physicochemical properties, mass, titratable acidity (TA), total soluble solids (TSS) and hue angle (h^*) of 'Satsuma' mandarin. Partial least squares (PLS) analysis gave accurate results for mass, TSS and h^* . The analysis showed that exclusion of spectra collected from styler-end and stem-end resulted in improved prediction models. The exclusion of styler-end and stem-end spectra, is therefore, an advantage as the two parts of the fruit may not contain much information about the fruit and therefore including them compromised quality of the information. When models developed from spectra of intact fruit were compared to models developed from peeled fruit, the removal of peel did not give an improvement which was attributed to heterogeneity of a peeled fruit surface and its transparency. OPLS-DA models were developed to distinguish between low and high classes of 'Satsuma' mandarin fruit, yielding accurate classification based on mass, TSS and h^* . Secondly, granulation in 'Navel' orange and seeds in 'Nadorcott' mandarin using X-ray CT based on radiographic images and tomographic images were investigated. Granulation was observed in 'Navel' orange radiographic and tomographic images. Accurate classification based on both image datasets was achieved. However, radiographic images could not reveal seeds in 'Nadorcott' mandarins. The tomographic images, in contrary, were able to reveal 'Nadorcott' seeds despite its inability to clearly separate the seeds from the endocarp of the fruit. The study demonstrated the potential of NIR spectroscopy and X-ray CT as possible non-destructive technologies for sorting of fruit based on physicochemical properties and internal structures respectively.

Acknowledgements

I would like to gratefully acknowledge the contributions of the following individuals and institutions:

- Prof U. L. Opara for lending expertise and guidance, for motivation and patience which enabled completion of this work.
- Dr H. H. Nieuwoudt for the continuous support, patience and enthusiasm which helped throughout the study. Proofreading of the chapters improved my scientific writing skill.
- Prof W. J. Perold for encouragement and patience throughout.
- Dr L. Magwaza for your guidance and helping in proofreading which helped in completion of the study.
- Special thanks to Prof B. M. Nicolai and P. Verboven, E. Herremans at MeBioS (Mechatronics, Biostatistics and Sensors) division of the Biosystems Department at K. U. Leuven University for granting me the opportunity to work in your research unit. Your warm welcome, support and guidance helped complete the research undertaken in your research unit.
- Fellow students in Postharvest Technology Research Lab at Stellenbosch University and MeBioS research unit at K. U. Leuven, your support does not go unnoticed. Special thanks to Dr Rebogile.
- My fellow colleagues at Agricultural Research Council (ARC) for your support and understanding.
- DST/NRF South African Research Chair Initiative (SARChI) and ARC for financial support.
- Lastly, thanks to my family, friends and significant other for your support and encouragement.

Preface

This thesis is presented as a compilation of chapters for purpose of publications where each chapter is an independent entity introduced separately. The referencing style is therefore in accordance with the requirements of Elsevier BV Publishers of Biosystems Engineering.

Contents

Abstract.....	iii
Acknowledgements.....	iv
Preface.....	v
Contents	vi
List of Published Peer-Reviewed Papers	ix
List of Conference Presentations	x
List of Figures	xi
List of Tables	xii
1. Introduction.....	1
References.....	4
2. Literature review	10
2.1 Introduction.....	10
2.2 Overview of citrus fruit quality.....	11
2.3 Non-destructive technologies for citrus quality measurements	11
2.4 Near infrared spectroscopy for fruit quality measurements.....	13
2.4.1 Position of sample during scanning	16
2.4.2 Radiation penetration	16
2.5 X-ray computed tomography for fruit quality measurement	17
2.5.1 X-ray radiation penetration and dosage	19
2.5.2 Performance of X-ray CT Scan.....	19
2.6 Conclusion	20
References.....	21

3. Detection of granulation in ‘Navel’ orange and ‘Nadorcott’ mandarin seeds using X-ray computed tomography	29
3.1 Introduction.....	29
3.2 Materials and methods	31
3.2.1 Citrus fruit.....	31
3.2.2 X-ray computed tomography	32
3.2.3 Image processing	32
3.2.4 Feature extraction.....	33
3.2.5 Histogram analysis.....	34
3.2.6 3D microstructural analysis	34
3.2.7 Classification.....	35
3.3 Results and discussion	36
3.3.1 Radiographic and tomographic images.....	36
3.3.2 Features of radiographic	39
3.3.3 Tomographic images.....	40
3.4 Conclusions.....	44
References.....	45
4. Classification of ‘Satsuma’ mandarin fruit based on physicochemical quality attributes using near infrared spectroscopy	50
4.1 Introduction.....	51
4.2 Materials and methods	53
4.2.1 Site and sample collection	53
4.2.2 NIR spectral acquisition.....	53

4.2.3 Physicochemical measurements.....	54
4.2.4 Data Analysis	55
4.3 Results and discussion	59
4.3.1 Spectral analysis.....	59
4.3.2 NIR based PLS calibration and validation models	60
4.3.3 Fruit classification with orthogonal partial least square-discriminant analysis	63
4.3.4 Additional analysis.....	68
4.4 Conclusion	69
References.....	69
5. General conclusions	74
5.1 Detection of granulation in ‘Navel’ orange and ‘Nadorcott’ mandarin seeds using X-ray computed tomography	74
5.2 Classification of ‘Satsuma’ mandarin fruit based on physicochemical quality attributes using near infrared spectroscopy	74

List of Published Peer-Reviewed Papers

van Dael, M., **Lebotsa, S.**, Herremans, E., Verboven, P., Sijbers, J., Opara, U. L., Cronje, P. J., & Nicolai, B. M. (2016). A segmentation and classification algorithm for online detection of internal disorders in citrus using X-ray radiographs. *Postharvest Biology and Technology*, 112, 205-214.

van Dael, M., Herremans, E., Verboven, V., Opara U. L., B. Nicolai & **Lebotsa, S.** (2016). Automated online detection of granulation in oranges using X-ray radiographs. *Acta Horticulturae*, 1119, 179 – 182.

List of Conference Presentations

Lebotsa, P. S., Magwaza, L., Opara, U. L., & Nieuwoudt, H. H. (2012). Chemometrics in the fruit industry, a benefit in postharvest technology. In *Second Convention of the South African Chemometrics Society*, Pretoria, South Africa, 7-11 May 2012.

List of Figures

Figure 3.1 X-ray equipment showing position of fruit during scanning.....	32
Figure 3.2 Conversion of radiographic images to tomographic images, slice of tomographic image reconstructed from NRecon (a) and 3D image (b).....	33
Figure 3.3 Radiographic and digital images of a healthy ‘Navel’ orange (a) and a granulated fruit (b) with corresponding digital images (top).....	37
Figure 3.4 Tomographic images of granulated ‘Navel’ orange (a) and ‘Nadorcott’ mandarin with seeds (b).....	38
Figure 3.5 Distribution of grey values for radiographic images (8-bit grey scale) of a granulated and a non-granulated ‘Navel’ orange fruit.....	41
Figure 3.6 3D images of granulated and non-granulated ‘Navel’ orange.....	43
Figure 4.1 NIR spectral acquisition setup showing the position of fruit during scanning, with fruit placed directly above the rotation integrating sphere to scan the stylar-end.	54
Figure 4.2 Summary of methodology comprising sample collection, scanning of samples, reference data collected, partial least squares (PLS) prediction models, orthogonal partial least squares-discriminant analysis (OPLS-DA) and analysis of variance (ANOVA). TSS is the total soluble solids, TA is titratable acidity, h^* is hue angle, OPLS-DA, Orthogonal partial least squares-discriminant analysis, PLS, Partial least squares, ANOVA, analysis of variance.	58
Figure 4.3 Typical raw Fourier transform NIR spectrum of one intact ‘Satsuma’ mandarin fruit in the wavelength range 800.44 nm – 2779.32 nm.	59
Figure 4.4 OPLS-DA plots, for TSS (a), h^* (b), and Mass (c), with scatter score plots on the left and corresponding S-line plots on the right. TSS classes L: 4 – 8°Brix, H: 9.1 – 15°Brix, h^* classes L: 60 – 75°, H: 75.1 – 120°, Mass classes L:23-60, H: 90-162.....	66

List of Tables

Table 2.1 Overview of non-destructive technologies applications in citrus fruit quality measurement	12
Table 2.2 Near infrared spectroscopy applications in citrus.....	14
Table 2.3 X-ray computed tomography applications in citrus.....	18
Table 3.1 Features of regions representing unaffected endocarp from radiographic images of ‘Navel’ oranges	34
Table 3.2 Description of 3-D morphometric parameters used to quantify the microstructure of apple tissue.....	35
Table 3.3 Mean and standard deviation for parameters of radiographs with and without granulation disorder, used as feature values for classification of ‘Navel’ oranges.....	39
Table 3.4 Classification results for classification of ‘Navel’ orange fruit according to granulated and non-granulated based on radiographic image features.....	40
Table 3.5 Range, mean and standard deviation (SD) for the histograms of granulated (n = 9) and non-granulated fruit, healthy (n=9), granulated (n = 21).	42
Table 3.6 Mean and standard deviation (SD) for 3D morphometric parameters of healthy and granulated ‘Navel’ orange samples.....	43
Table 3.7 Classification results for classification of ‘Navel’ orange fruit according to granulation and non-granulation based on 3D morphometric parameters.....	44
Table 4.1 PLS model statistics for 6, 4 and 1 scanning positions) as determined from NIR spectra and reference physicochemical measurements	62
Table 4.2 Range, mean and standard deviation (SD) for mass, TSS and h* for two sets of classes of each of the quality parameters. Values for comparing the two classes for each quality attribute are reported with different letters next to them in the same column.	64
Table 4.3 ‘Satsuma’ mandarin OPLS-DA classification table for test set validation according to low (L) and high values (class H) of TSS and h*	65

1. Introduction

Fruits are generally known to have nutritional value due to their beneficial components such as vitamins, sugars, antioxidants, and other components such as minerals and acids (Cassano et al., 2003; Topuz et al., 2005; Vicente et al., 2009). Because of these important nutritional components, fruits play an important role in a healthy human diet, although nutritional value varies depending on the type of fruit, cultivar and maturity stage (Vicente et al., 2009). Citrus fruits are well known for high vitamin C content, also known as ascorbic acid, which plays medicinal role such as prevention of scurvy (Schrock et al., 2008) and increase of body resistance to infection (Njoku et al., 2011) amongst other benefits.

Citrus is an important fruit crop in the world grown in 140 countries (Iglesias et al., 2007; Molto & Blasco, 2008; Liu et al., 2012;). Citrus production in South Africa has shown an annual increase over the past years from 2008/2009 to 2012/2013, with a production of 2, 343, 016 tons in 2012/2013 (DAFF, 2013). The South African citrus industry contributed approximately R6.9 billion to the total gross value of South African agricultural production during the 2010/2011 production season (DAFF, 2012).

Various citrus cultivars are grown in many regions across South Africa, including Limpopo, Western Cape, Mpumalanga, KwaZulu-Natal and Northern Cape provinces (DAFF, 2012; CGA, 2010). There are several cultivars classified as citrus, which include among others, mandarins (cultivars include Satsuma, Clementine and Nadorcott) , oranges (cultivars include Navel and Valencia), lemons, limes (cultivars include Eureka), tangerines and grapefruit (Molto & Blasco, 2008). Citrus fruit typically consists of segments in which juice segments and seeds grow, peel (divided into flavedo and albedo), and the central axis which form core of the fruit (Iglesias et al., 2007; Ladaniya, 2008; Liu et al., 2012).

Quality affects citrus fruit market value (Kotwaliwale et al., 2014). The quality of citrus fruit is mainly affected by factors such as temperature, humidity, water stress, chemicals and handling practices amongst others (Ladaniya, 2008; Sela & Fallik, 2009; Bermejo & Cano, 2012). When these conditions are unfavourable physiological disorders may result (Lee et al., 2015). The citrus industry is faced with such challenges/threats of fruit disorders which affect quality of citrus fruit and its market value (Sharma et al., 2006; Ladaniya, 2008; DAFF, 2010). These include preharvest disorders such as fruit splitting/cracking, rind pitting, sunburn, freeze injury and postharvest disorders such as chilling injury, granulation, rind staining and rind breakdown among others (Ladaniya, 2008; Magwaza et al., 2012; Lee et al.,

2015; Wang et al., 2014). Ladaniya (2008) further reports that some of these disorders have visible symptoms and recommended control measures, while some do not have visible external symptoms. DAFF (2012) reported that the South African citrus production is mainly aimed at the export market. In addition, presence of seeds has shown to negatively impact to consumer acceptability (Raza, 2003).

In addition to the presence of disorders and seeds, the internal quality in terms of chemical composition such as sugar content and acidity is also an important factor to market value (McGlone et al., 2003; Gomez et al., 2006). Consumer acceptance studies on fruits such as peach, nectarine, cherries and kiwi reflect total soluble solids (TSS) and total acidity (TA) as important quality parameters (Crisosto & Crisosto, 2001; Crisosto, et al., 2003; Crisosto et al., 2004; Crisosto & Crisosto, 2005). McGlone et al. (2003) reported that TSS and TA are important internal quality parameters for 'Satsuma' mandarin. This is reflected in New Zealand's export grade standards, where sugar to acid ratio is reflected as a measure for consumer preference of Satsuma mandarin. Katz et al. (2007) also reported that TSS and TA are key fruit quality determinants and are used to determine whether the fruit can be marketed.

Shewfelt (2009) and Magwaza & Opara (2015) reported that the internal quality in terms of flavour (which is a function of TSS and TA) determines consumer satisfaction. It is, therefore, necessary to be able to measure fruit quality in terms of presence of disorders, presence of seeds and chemical information such as TSS and TA before they are sent for market. Gomez et al. (2006) highlighted that the citrus industry requires high quality inspection on a large scale due to the high production of citrus fruit. It is therefore vital that produce should be monitored to meet quality standards.

There are various techniques used in the food industry for quality evaluation. There is still ongoing research to improve the use and accuracy of the use of such techniques. Evaluation techniques are divided into destructive as well as non-destructive methods, the latter being of more advantage than the former (Lurie, 2009; Magwaza et al., 2013a, c). Destructive methods involve taking or extracting a representative sample from a batch or consignment, testing and discarding the sample (Nicolai et al., 2009). The main disadvantage of the non-destructive methods is that the 'representative' sample may not be representative due to variations of fruits as a result of variation in maturity stage, position in canopy and other environmental factors (Guthrie et al., 2005; Golic & Walsh, 2006; Louw & Theron, 2010; Magwaza et al.,

2013b, c). Non-destructive methods, on the other hand, allow measurements of individual without extracting and discarding samples (Lurie, 2009; Nicolai et al., 2009; Magwaza et al., 2013a). It is for this reason that in recent years the focus has been placed mainly on non-destructive measuring techniques (Abott, 1999; Molto & Blasco, 2008).

The non-destructive techniques that are currently available for laboratory and sometimes commercial quality assessment include hyperspectral Imaging (Lu, 2008), magnetic resonance imaging (MRI) (Abbott, 1999; Musse et al., 2009; Nicolai, et al., 2009), optical coherence tomography (OTC) (Magwaza et al., 2013a), X-ray Computed Tomography (X-ray CT) (Herremans et al., 2014; Magwaza & Opara, 2014), X-ray radiography (Abbott, 1999), Linescan radiography (Abbott, 1999), and visible to near infrared (NIR) spectroscopy (Vis/NIRS) (Guthrie et al., 2005; Gomez et al., 2006; Nicolai et al., 2007; Liu, et al., 2010; Louw & Theron, 2010; Magwaza et al., 2012; de Oliveira et al., 2014; Magwaza et al., 2014a, b; Maniwaru et al., 2014).

Studies on NIR technique have revealed the potential of the technique to measure internal quality attributes (Perez-Marin et al., 2009). The main advantages of NIRS are that it allows non-destructive analysis and allows multicomponent analysis i.e. allows simultaneous measurement of several parameters (de Oliveira et al., 2014). Amongst the imaging techniques, X-ray CT has been reported to have a capability of obtaining very high resolution images of the internal structure of plant material's cellular and subcellular structure (Nicolai et al., 2009).

In this thesis, NIR spectroscopy and X-ray CT are investigated for non-destructive assessment of citrus fruit quality. NIRS is used to investigate the effect position of 'Satsuma' mandarin fruit during scanning on prediction models accuracies. X-ray CT is also investigated for detection of granulation disorder in 'Navel' orange as well as seeds in 'Nadorcott' mandarin. Furthermore, classification of fruit using NIR spectroscopy and X-ray CT based on physicochemical properties and internal structures respectively, is investigated. Additional analysis is done on effect of peel on prediction models for physicochemical quality parameters of 'Satsuma' mandarin.

References

- Abbott, J. A. (1999). Quality measurement of fruits and vegetables. *Postharvest Biology and Technology*, 15, 207–225.
- Bermejo, A., & Cano, A. (2012). Analysis of nutritional constituents in twenty citrus cultivars from the Mediterranean area at different stages of ripening. *Food and Nutrition Sciences*, 3, 639-650.
- Cassano, A., Drioli, E., Galaverna G., Marchelli, R., Di Silverstro, G., & Cagnasso, P. (2003). Clarification and concentration of citrus and carrot juices by integrated membrane processes. *Journal of Food Engineering*, 57, 153-163.
- Citrus Growers' Association (CGA). (2010). Key industry statistics, Hillcrest, South Africa. <http://www.lona.co.za/pdf/full-industry-statistics-2010.pdf> (last accessed on 09.03.15).
- Crisosto, C. H., & Crisosto, G. M. (2001). Understanding consumer acceptance of early harvested 'Hayward' kiwifruit. *Postharvest Biology and Technology*, 22, 205-213.
- Crisosto, C. H., Crisosto, G. M., & Metheney, P. (2003). Consumer acceptance of 'Brooks' and 'Bing' cherries is mainly dependent on fruit SSC and visual skin color. *Postharvest Biology and Technology*, 28, 159-167.
- Crisosto, C. H., Garnera, D., Crisosto, G. M., & Bowerman, E. (2004). Increasing 'Blackamber' plum (*Prunus salicina* Lindell) consumer acceptance. *Postharvest Biology and Technology*, 34, 237-244.
- Crisosto, C. H., & Crisosto, G. M. (2005). Relationship between ripe soluble solids concentration (RSSC) and consumer acceptance of high and low acid melting flesh peach and nectarine (*Prunus persica* (L.) Batsch) cultivars, *Postharvest Biology and Technology*, 38, 239–246.
- de Oliveira, G. A., Bureau, S., Renard, C. M. C., Pereira-Netto, A. B., & de Castilhos, F. (2014). Comparison of NIRS approach for prediction of internal quality traits in three fruit species. *Food Chemistry*, 143, 223-230.
- Department of Agriculture, Forestry and Fisheries (DAFF). (2010). A profile of the South African citrus market value chain, Pretoria, South Africa.

<http://www.daff.gov.za/docs/AMCP/CitrusMVCP2010-11.pdf> (last accessed on 09.03.15).

Department of Agriculture, Forestry and Fisheries (DAFF). (2012). A profile of the South African citrus market value chain, Pretoria, South Africa. <http://www.nda.agric.za/docs/AMCP/Cmvp2012.pdf> (last accessed on 09.03.15).

Department of Agriculture, Forestry and Fisheries (DAFF). (2013). Trends in the Agricultural sector, Pretoria, South Africa. <http://www.econostatistics.co.za/TrendsinSAAgriculture13.pdf> (last accessed on 18.04.2015).

Golic, M., & Walsh, K. B. (2006). Robustness of calibration models based on near infrared spectroscopy for the in-line grading of stonefruit for total soluble solids content. *Analytica Chimica Acta*, 555, 286-291.

Gomez, G. H., He, Y., & Pereira, A. G. (2006). Non-destructive measurement of acidity, soluble solids and firmness of Satsuma mandarin using Vis/NIR-spectroscopy techniques. *Journal of Food Engineering*, 77, 313–319.

Guthrie, J. A., Walsh, D. J., Reid, D. J., & Liebenberg, C. J. (2005). Assessment of internal attributes of mandarin fruit 1. NIR calibration model development. *Australian Journal of Agricultural Research*, 56, 405-416.

Herremans, E., Verboven, P., Defraeye, T., Rogge, S., Ho, Q. T., Hertog, et al. (2014). X-ray CT for quantitative food microstructure engineering: The apple case. *Nuclear Instruments and Methods in Physics Research B*, 324, 88-94.

Iglesias, D. J., Cercos, M., Jose M., Flores, C., Naranjo, M. A., Ríos, G., Carrera, E., Rivero, O. R., Lliso, I., Morillon, R., Tadeo, F. R., & Talon, M. (2007). Physiology of citrus fruiting. *Brazilian Journal of Plant Physiology*, 19, 333-362.

Katz, E., Fon, M., Lee, Y. J., Phinney, B. S., & Sadka, A. (2007). The citrus fruit proteome: insights into citrus fruit metabolism, *Planta*, 226, 989-1005.

Kotwaliwale, N., Singh, K., Kalne, A., Jha, S. N., Seth, N., & Kar, A. (2014). X-ray imaging methods for international quality evaluation of agricultural produce. *Journal of Food Science and Technology*, 51, 1-15.

- Ladaniya, M. S. (2008). Preharvest factors affecting fruit quality and postharvest life. In: Citrus fruit: Biology, technology and evaluation, Elsevier Inc., London, UK.
- Lee, T. C., Zhong, P. J., & Chang, P. T. (2015). The effects of preharvest shading and postharvest storage temperatures on the quality of 'Ponkan' (*Citrus reticulata* Blanco) mandarin fruits. *Scientia Horticulturae*, 188, 57-65.
- Liu, Y., Sun, X., Zhang, H., & Aiguo, O. (2010). Nondestructive measurement of internal quality of Nanfeng mandarin fruit by charge coupled device near infrared spectroscopy. *Computers and Electronics in Agriculture*, 71S, S10–S14.
- Liu, Y. U., Heying, E. & Tanumihardjo, S. A. (2012). History, global distribution, and nutritional importance of citrus fruits. *Comprehensive Reviews in Food Science and Food Safety*, 11, 530 - 545
- Louw, E. D., & Theron, K. I. (2010). Robust prediction models for quality parameters in Japanese plums (*Prunus salicina* L.) using NIR spectroscopy. *Postharvest Biology and Technology*, 58, 176–184.
- Lu, R. (2008). Quality evaluation of Fruit by Hyperspectral Imaging. In: Computer Vision Technology for Food Quality Evaluation, Elsevier Inc, East Lansing , USA.
- Lurie, S. (2009). Quality parameters of fresh fruit and vegetable at harvest and shelf life. In: Optic Monitoring of Fresh and Processed Agricultural Crops, Taylor & Francis Group, Florida, USA.
- Magwaza, L. S., Opara, L. U., Terry, L. A., Landahl, S., Cronje, P. J., Nieuwoudt, H., Mouazen, A. M., Saeys, W., & Nicolai, B. M. (2012). Prediction of 'Nules Clementine' mandarin susceptibility to rind breakdown disorder using Vis/NIR spectroscopy. *Postharvest Biology and Technology*, 74, 1-10.
- Magwaza, L. S., Ford, H. D., Cronje, P. J. R., Opara, U. L., Landahl, S., Tatam, R. P., & Terry, A. T. (2013a). Application of optical coherence tomography to non-destructively characterize rind breakdown disorder of 'Nules Clementine' mandarins. *Postharvest Biology and Technology*, 84, 16-21.

- Magwaza, L. S., Opara, U. L., Cronje, P. J. R., Landahl, S., & Terry, L. A. (2013b). Canopy position affects rind biochemical profile of 'Nules Clementine' mandarin fruit during postharvest storage. *Postharvest Biology and Technology*, 86, 300-308.
- Magwaza L. S., Opara, U. L., Terry, L. A., Landahl, S., Cronje, P. J. R., Nieuwoudt, H. H., Hanssens, A., Saeys, W., & Nicolai, B. M. (2013c). Evaluation of Fourier transform-NIR spectroscopy for integrated external and internal quality assessment of Valencia oranges. *Journal of Food Composition and Analysis*, 31, 144-154.
- Magwaza, L. S., Opara, U. L., Cronje, P. J. R., Landahl, S., Nieuwoudt, H. H., Mouazen, B. M. N., & Terry, L. A. (2014a). Assessment of rind quality of 'Nules Clementine' mandarin during postharvest storage: 1. Vis/ NIRS PCA models and relationship with canopy position. *Scientia Horticulturae*, 165, 410-420.
- Magwaza, L. S., Opara, U. L., Cronje, P. J. R., Landahl, S., Nieuwoudt, H. H., Mouazen, A. M., Nicolai, B. M., & Terry, L. A. (2014b). Assessment of rind quality of 'Nules Clementine' mandarin during postharvest storage: 2. Robust Vis/NIRS PLS models for prediction of physio-chemical attributes. *Scientia Horticulturae*, 165, 421-432.
- Magwaza, L. S., & Opara, U. L. (2014). Investigating non-destructive quantification and characterization of pomegranate fruit internal structure using X-ray computed tomography. *Postharvest Biology and Technology*, 95, 1-6.
- Magwaza, L. S., & Opara U. L. (2015). Analytical methods for determination of sugars and sweetness of horticultural products – A review. *Scientia Horticulturae*, 184, 179-192.
- Maniwaru, P., Nakano, K., Boonyakiat, D., Ohashi., S., Hiroi, M., & Tohyama, T. (2014). The use of visible and near infrared spectroscopy for evaluating passion fruit postharvest quality. *Journal of Food Engineering*, 143, 33-43.
- McGlone, A. V., Fraser, D. G., Jordan, R. B., & Kunemeyer, R. (2003). Internal quality assessment of mandarin fruit by vis/NIR spectroscopy. *Near Infrared spectroscopy*, 11, 323-332.
- Molto, E., & Blasco, J. (2008). Computer vision technology for food quality evaluation. Quality evaluation of citrus fruit, pp 243-264. Valencia, Spain: Elsevier Inc.

- Musse, M., Quellec, S., Devaux, M. F., Cambert, M., Lahaye, M., & Mariette, F. (2009). An investigation of the structural aspects of the tomato fruit by means of quantitative nuclear magnetic resonance imaging. *Magnetic Resonance Imaging*, 27, 709-719.
- Nicolai, B. M., Beullens, K., Bobelyn, E. Peirs, A., Saeys, W., Theron, K. I., & Lammertyn, J. (2007). Nondestructive measurement of fruit and vegetable quality by means of NIR spectroscopy: A review, *Postharvest Biology and Technology*, 46, 99-118.
- Nicolai, B. M., Bulens, I., Josse De Baerdemaeker, De Ketelaere, B., Hertog, M. L. A. T. M., Verboven, P., et al. (2009). Non-destructive evaluation: Detection of external and internal attributes frequently associated with quality and damage. In: *Postharvest Handling: A Systems Approach*, Elsevier, London, UK.
- Njoku, P. C., Ayuk, A. A., & Okoye, C. V. (2011). Temperature effects on Vitamin C content of citrus fruits. *Pakistan Journal of Nutrition*, 10, 1168-1169.
- Raza, H., Khan, M. M., & Khan, K. K. (2003). Seedlessness in citrus. *International Journal of Agriculture and Biology*, 5, 388-391.
- Perez-Marin, D., Sanchez, M. T., Paz, P., Soriano, M. A., Guerrero, J. E., & Garrido-Varo, A. (2009). Non-destructive determination of quality parameters in nectarines during on-tree ripening and postharvest storage, *Postharvest Biology & Technology*, 52, 180-188.
- Sela, S., & Fallik, E. (2009). Microbial quality and safety of fresh produce, *Postharvest Handling: A Systems Approach* (second edition), 351-398.
- Schrock, D., Walheim, L., More, P., & Sweet, C. (2008). All about citrus and subtropical fruits. 2nd ed. USA: The Scotts Company.
- Sharma, R. R., Singh, R., & Saxena, S. K. (2006). Characteristics of citrus fruits in relation to granulation. *Scientia Horticulturae*, 111, 91-96.
- Shewfelt, R. L. (2009). Measuring quality and maturity. In: *Postharvest and Handling: A system approach*, 461-481.
- Topuz, A., Topakci, M., Canakci, M., Akinci, I., & Ozdemir, F. (2005). Physical and nutritional properties of four orange varieties. *Journal of Food Engineering*, 66, 519-523.

Vicente, A. R., Manganaris, G. A., Sozzi, G. O., & Crisosto, C. H. (2009). Nutritional Quality of Fruits and Vegetables. In: Postharvest Handling: A Systems Approach (second edition), 57-106.

Wang, X. Y., Wang, P., Qi, Y. P., Zhou, C. P., Yang, L. T., Liao, X. Y., Wang, L. Q., Zhu, D. H., & Chen, L. S. (2014). Effects of granulation on organic acid metabolism and its relation to mineral elements in *Citrus grandis* juice sacs, *Food Chemistry*, 145, 984-990.

2. Literature review

2.1 Introduction

Citrus fruit quality is of major concern due to its impact on citrus production and market value (Xudong et al., 2009; Liu et al., 2010; Chen et al., 2013). As a result, there is an increasing need to determine fruit external and internal qualities due to required levels of acceptance in the market and quality standards in terms of a combination of quality attributes such as soluble solids content, acidity, firmness, freedom from external or internal defects (Chen et al., 2013). For example, Department of Agriculture, Forestry and Fisheries provides quality standards for various citrus varieties (DAFF, 2012; DAFF, 2016)

Research has recently been focused on the development of non-destructive techniques for measuring quality parameters of different agricultural commodities (Abu-Khalaf & Bennedsen, 2004). This is due to the fact that the use of non-destructive measuring techniques assures quality while measured fruit remains whole, and therefore may increase consumer satisfaction and acceptance (Omar & MatJafri, 2009). There is a wide range of non-destructive techniques utilised in the fruit industry. The techniques include spectroscopic methods such as near infrared (NIR) spectroscopy, fluorescence spectroscopy, Nuclear Magnetic Resonance (NMR) and imaging systems such as X-ray computed tomography (X-ray CT), optical coherence tomography (OCT), hyperspectral imaging (HSI), fluorescence imaging (FI) and magnetic resonance imaging (MRI) among others (Chen et al., 2013; Magwaza et al., 2013a; Nicolai et al., 2014). These techniques have been applied on different types of fruit for measurement of physicochemical quality parameters and assessment of fruit disorders (Abbott, 1999; Lu, 2008; Musse et al., 2009; Nicolai et al., 2009; Magwaza et al., 2013a; Magwaza & Opara, 2014).

Amongst the non-destructive methods are NIR spectroscopy and X-ray computed tomography, which are specifically applicable in analysing the physicochemical attributes and analysis of fruit internal physical disorders respectively. Overall, NIR spectroscopy, which can be applied to evaluate fruit physicochemical characteristics, may be favoured over other non-destructive techniques as it requires no sample preparation and can be used to analyse samples with high moisture content whilst simultaneously examine several sample's constituents (Huang et al., 2008). With reference to imaging, X-ray CT has the capability to obtain high resolution images of internal structures of fruit (Nicolai et al., 2009) and has the

advantage of adapting to online measurements (Abbot, 1999). Following that, its large field of view makes it feasible to analyse whole fruit without sample preparation (Leornard et al., 2008).

Several reviews of these techniques are available. Magwaza et al. (2012) reviewed the general aspects of NIRS applied to citrus fruit. The objective of this chapter is to review non-destructive technologies in relation to citrus fruit quality measurements and in particular the NIR spectroscopy and X-ray CT for non-destructive quality evaluation of citrus fruit.

2.2 Overview of citrus fruit quality

The meaning and perception of quality is different for different people (Ladaniya, 2008) and different groups in the supply chain, from farmers to consumers (Friebel et al., 2009). For some consumers good quality can mean good external appearance and taste (Kader, 2002). Abbott (1999) indicated that quality parameters of fruit include sensory attributes (appearance, texture, aroma and taste), nutritional constituents, chemical and mechanical properties and disorders. Fruit quality can therefore be defined as the combination of attributes that have more importance in determining degree of consumer acceptance (Ladayina, 2008).

2.3 Non-destructive technologies for citrus quality measurements

Non-destructive technologies which have been applied in citrus fruit quality determination include NIR spectroscopy (Ncama et al., 2017), MRI (Hernandez-Sanchez et al., 2006; Barreiro et al., 2008), HSI (Li et al., 2016), OCT (Magwaza et al., 2013a) and X-ray CT (van Dael et al., 2016). NIR spectroscopy has been applied for determination of total soluble solids (TSS) and dry matter (DM) in ‘Imperial’ mandarin (Guthrie et al., 2005a, b), in ‘Satsuma’ mandarins for firmness, TSS, and pH (Gomez et al., 2006). The technique has proved to yield accurate models for predicting the physicochemical quality attributes. X-ray CT has been applied in ‘Navel’ orange and ‘Eureka’ lemon (van Dael et al., 2016) and has shown ability to detect granulation and endoxerosis when radiographic images were used. Table 2.1 below gives an overview of non-destructive technologies which have been applied for citrus fruit quality evaluation.

Table 2.1 Overview of non-destructive technologies applications in citrus fruit quality measurement

Technique	Applications in citrus fruit	References
NIR	Prediction of TSS, TA, and TSS: TA ratio, pH, DM, mass, equatorial diameter, colour parameters (L*, a*, b*, C*, h* and CI), firmness, juice weight, juice content, MI	McGlone et al. (2003), Guthrie et al. (2005a), Guthrie et al. (2005b), Gomez et al. (2006), Jamshidi et al. (2012), Sanchez et al. (2013), Ncama et al. (2017), Magwaza et al. (2014b), Magwaza et al. (2014c), Wang et al. (2014)
HSI	Detection of the early symptoms of decay	Li et al. (2016)
MRI	Detection of seeds	Hernandez-Sanchez et al. (2006); Barreiro et al. (2008)
X-ray CT	Detection of granulation and endoxerosis	van Dael et al. (2016)

2.4 Near infrared spectroscopy for fruit quality measurements

Spectroscopy is the use of the absorption, emission, or scattering of electromagnetic radiation by matter to qualitatively or quantitatively study the matter or to study physical processes. Near infrared radiation is found between the visible and infrared region of the electromagnetic spectrum, and is characterized as the region from 780nm to 2500nm (Schwanninger et al., 2011; Miller & Miller, 2010; Huang et al., 2008). Optical properties (reflectance, transmittance, absorbance or scatter of radiation) of horticultural commodities have shown their response to radiation in the near infrared region (Abbott, 1999). The NIR is characterized by absorption bands caused by stretching vibrations of molecular groups such as C-H, O-H and N-H (Schwanninger et al., 2011; Nicolai et al., 2014). Constituents associated with the molecular groups such as starch, sugars, alcohol, acids, moisture and proteins which can be quantified using NIRS (Abu-Khalaf & Bennedsen, 2004; Nicolai et al., 2014).

Known advantages of NIR spectroscopy include the non-destructive nature, its ability to measure samples with high moisture content, the fact that there is no need for sample preparation and simultaneous measurement of multiple attributes such as total soluble solids, pH and acid levels (Huang et al., 2008). One of the challenges with regard to application of NIRS for continuous monitoring of products is the need for robust calibration models which are stable and reliable for accurate measurements (Huang et al., 2008).

NIRS has been successfully applied for determination of quality parameters of a variety of fruit (Peirs et al., 2003; Nicolai et al., 2007, Jha & Matsuoka, 2000). The technique has been successfully applied to study internal qualities of various fruits such as mandarins (McGlone et al., 2003; Guthrie et al., 2005a,b; Gomez et al., 2006; Liu et al., 2010; Sanchez et al., 2013; Magwaza et al., 2014a, b), oranges (Cayuela 2008; Cayuela & Weiland, 2010; Jamshidi et al., 2012; Magwaza et al., 2013; Wang et al., 2014), plums (Louw and Theron, 2010; Perez-Marin et al., 2010), apples (Bobelyn et al., 2010), dates (Mabood et al., 2015), and mango (Rungpichayapichet et al., 2016). The technique has been used for determination of quality parameters such as total soluble solids (TSS), total acidity (TA), juice content, colour and firmness amongst others. Table 2.2 summarises quality measurements using NIR done on citrus and key findings by different researchers.

Table 2.2 Near infrared spectroscopy applications in citrus

Cultivar	Quality parameters	Key findings	Reference
'Satsuma' mandarin	TSS, TA	SSC was predicted well with transmission mode in the wavelength of 700 nm – 930 nm compared to interactance and reflectance. TA was not well predicted by all the three modes.	McGlone et al. (2003)
'Satsuma' mandarin	TSS, pH and compression force.	Better models were obtained with MSC pre-processing method, PLS gave slightly better results compared to PCR.	Gomez et al. (2006)
'Imperial' mandarin	TSS and DM	Better results for TSS were obtained with spectra from equatorial and distal spots of the fruit than proximal end. There was no significant difference between models developed from interactance and transmittance measurements.	Guthrie et al. (2005a)
'Imperial' mandarin	TSS and DM	Models were less robust across seasons than locations and time within a season. Adding more samples improved prediction.	Guthrie et al. (2005b)
'Clemevilla' mandarin	Mass, equatorial diameter, L*, a*, b*, C*, h*, CI, firmness, Maximum penetration force, juice weight, juice content, SSC, pH, TA, MI	pH was well predicted, $R^2 = 0.61$. All other parameters were not well predicted, $R^2 < 0.60$, described by authors as control limit. The reasons for low prediction accuracy include insufficient number of samples removed as outliers in some quality attributes. For firmness low prediction was attributed to low penetration depth of NIR, especially for measurements made to a puncturing depth of 10 mm.	Sanchez et al. (2013)

Cultivar	Quality parameters	Key findings	Reference
'Nules' Clementine	Rind hue angle, Fruit weight loss and rind dry matter	PCA on laboratory reference measurements and on vis/NIR spectrum showed variation between fruit harvested from different canopy positions. Carbohydrates, weight loss and canopy position were positively correlated to rind breakdown.	Magwaza et al. (2014b)
'Nules' Clementine	Incidence of RBD, h*, rind colour, rind dry matter, sucrose, glucose and fructose	PLS results showed potential of vis/NIR to predict rind physic-chemical attributes after storage. Combining data from different orchards improved prediction accuracy. Combining data from different seasons reduced prediction accuracy. Models developed using combined orchards and seasons gave better model statistics than using a single orchard or a single season.	Magwaza et al. (2014c)
'Valencia' oranges	SSC, TA, SSC/TA, BrimA	PLS gave slightly better models than PCR for all the quality parameters	Jamshidi et al. (2012)
'Navel' orange	SSC	Involvement of VIS region degraded performances of PLS models. This was attributed to VIS region containing mainly colour information, chlorophyll content. Comparing models developed on unpeeled to peeled orange, better models were achieved with unpeeled in interactance and reflectance, while better results were obtained with peeled spectra in transmittance modes.	Wang et al. (2014)

2.4.1 Position of sample during scanning

The position of sample during scanning or the point at which fruit is scanned affects the accuracy of calibration models (Walsh, 2005; Guthrie et al., 2005a, b). This is due to variation in quality parameters of interest such as TSS in fruit. Walsh (2005) reported that accuracy of NIR spectroscopy is limited by non-homogeneity of the attribute of interest in the fruit. Guthrie et al. (2005a) compared model performance based on the point on which fruit is scanned with NIR instrument and found that the proximal end (stem-end) gave poor prediction model when compared to the equatorial and distal (stem-end). Wang et al. (2014) in their study scanned the fruit along the equatorial positions.

2.4.2 Radiation penetration

The penetration of radiation inside fruit depends on the chemical composition and optical properties related to structure of the sample (Meinke & Friebel, 2009; Cozzolino et al., 2011). The penetration is also dependent on wavelength (Saad et al., 2014). NIR has limited penetration depth and depends on variety on which the measurements are taken (Lammertyn et al., 2000). Several authors have studied the penetration of radiation inside fruit such as mandarin (Fraser et al., 2003), 'Navel' orange (Wang et al. 2014) and apple (Lammertyn et al., 2000). Lammertyn et al. (2000) studied the penetration depth of NIR in relation to wavelength in apple. The study showed that there is high penetration of up to 4 mm in the shorter wavelength, 700 – 900 nm compared to penetration depth of 1 to 3 mm in the wavelength range of 900 – 1900 nm. Fraser et al. (2003) studied the distribution of light inside mandarin fruit during internal quality assessment by NIR spectroscopy. The results showed that there is rapid reduction in light level across skin of mandarin fruit and less rapid as it continues into the endocarp. This indicated that the peel region of mandarin fruit attenuates more radiation compared to the endocarp. Fraser et al. (2003) added that the peel of mandarin fruit has significant internal reflective properties.

2.5 X-ray computed tomography for fruit quality measurement

The application of X-ray technologies began with medical imaging, geology, and engineering (Mees et al., 2003; Kotwaliwale et al., 2014). The X-ray CT is also commonly used in airports for inspection (Jiang et al., 2008; Kotwaliwale et al., 2014). The technology is now being applied in agricultural and food industries for inspection purposes (Jha & Matsuoka, 2000). Existing researches include detection of split pit of peaches (Ogawa et al., 2003), injuries inside fruit as a result of pests (Lin *et al.*, 2005; Jiang *et al.*, 2008; Lin et al., 2008; Haff & Pearson, 2007; Chuang et al., 2011), core breakdown in pears (Lammertyn et al., 2003a; Lammertyn et al., 2003b); browning disorder in apple (Herremans et al., 2013; Herremans et al., 2014a), watercore disorder in apple (Herremans et al., 2014b), quantification of volumes in pomegranate (Magwaza & Opara, 2014), to visualise changes in mango during ripening (Cantre et al., 2014) and in citrus for detection of internal disorders (Peiris et al., 1998; van Dael et al., 2016). Table 2 summarises fruit quality measurements by X-ray CT on fruit and key findings by different researchers.

Table 2.3 X-ray computed tomography applications in citrus

Cultivar	Quality parameters	Key findings	Reference
'Washington Navel' orange and 'Eureka' lemons	To develop a robust and fast image processing and classification algorithm to detect granulation in oranges and endoxerosis in lemons	A naive Bayesian classifier was developed for identifying granulation in oranges and endoxerosis in lemons from X-ray radiographs, which can be implemented in existing online X-ray radiograph systems.	van Dael et al. (2016)
Citrus, peach and guava	To design and implement a thresholding algorithm to segment infestation (cavity/pest) in X-ray images	Algorithm for processing X-ray images for determination of infestation sites of a fruit was developed. The algorithm was successfully tested on x-ray images of peach and guava.	Jiang et al. (2008)

2.5.1 X-ray radiation penetration and dosage

Penetration and attenuation of x-ray radiation depends on composition, density and thickness of the material (Jiang et al., 2008). The interest in application of X-ray radiation in food has led to enormous research on its effect. Proteins, carbohydrates, and fats in food have been found to be relatively stable when irradiated up to 10 kGy (Roberts & Weese, 1995). Minerals such as Vitamin C however have been found to be susceptible to irradiation dosage of 1 kGy or more. In the United States, the use of X-ray radiation for food has been approved at a dose of ≤ 1.0 kGy (FDA, 1986; Alonso et. al., 2007).

2.5.2 Performance of X-ray CT Scan

The performance of CT scanner that ultimately affects image quality is affected by factors such as radiation dose, resolution noise (Goldman, 2007). There are also several trade-offs existing between the parameter settings (such as voltage, current, exposure time) and the different aspects of image quality (such as contrast and artefacts).

Voltage and current determines the power and intensity of X-ray radiation, hence penetration into an object (Quinn et al., 1980). Therefore the quality of the X-ray image depends on the voltage and current settings (Jiang et al., 2008). The setting for voltage must be as low as possible for soft materials and current at maximum of the selected voltage (Quinn et al., 1980; Jiang et al., 2008). Maximum current helps produce enough photons for the sensor elements to detect (Jiang et al., 2008).

Frame averaging is a technique to get better statistics, that is, more image data or a better signal to noise ratio (SNR) in your images. The beam does not stay on any one spot as long, but rather revisits each spot for several scans, with each scan being averaged with the ones before it. Increased acquisition time due to the accumulation of delays is inherent in each line-scan

Suitable X-ray spectra filtration such as Aluminium and Copper may be mounted in the X-ray beam near the X-ray tube, before penetration of the X-ray photons into an object to filter low energy radiation that may result in beam hardening artefact from entering the object (Ay & Zaidi, 2006; Quinn et al., 1980). Quinn (1980) further explains that the metallic filter may adequately serve the purpose of eliminating overexposure in the thin regions of the specimen and in the area surrounding the part (the edge) and therefore reduction/elimination of beam

hardening. MG (2011) and Quinn (1980) suggest that for soft material/tissues, the low energy X-rays are the X-rays attenuated and generally such low energy radiation does not cause beam hardening and therefore requires no filtration.

Beam hardening is an artefact that is identified by the same material appearing darker in the centre of the image than in the periphery (Goldman, 2007) i.e. the edge of the scanned object appearing brighter than the rest of the object even though the density does not vary entirely with other areas within the object. This artefact is caused by the polyenergetic nature of X-ray radiation, and result from low energy X-rays being absorbed as the X-rays pass through an object (Ay & Zaidi, 2006). X-Rays produced in x-ray tubes cover a broad continuum of energies, up to a maximum numerically equal to the x-ray tube kilovoltage, hence they are referred to as polyenergetic/ polychromatic (Goldman, 2007; Quinn et al., 1980). Beam hardening does not appear in softer materials where low energy X-rays are used, since the low energy radiation is the energy that is attenuated (GM, 2011).

2.6 Conclusion

The review has shown potential of NIR spectroscopy and X-ray CT as non-destructive technologies for internal measurements of physicochemical and internal structure of citrus fruit. Various studies on citrus have found accurate predictions using NIR spectroscopy of majority of physicochemical quality parameters such as sugar content, acid content, fruit colour and mass, to mention a few. X-ray CT has also shown the potential to reveal information of internal structure of citrus fruit based on radiographic images.

References

- Abbott, J. A. (1999). Quality measurement of fruits and vegetables. *Postharvest Biology and Technology*, 15, 207–225.
- Abu-Khalaf, N., & Bennedsen, B. S. (2004). Near infrared (NIR) technology and multivariate data analysis for sensing taste attributes of apples. *International Agrophysics*, 18, 203 – 211.
- Alonso, M., Palou, L., del Rio, M. A., & Jacas, J. A. (2007). Effect of X-ray irradiation on fruit quality of Clementine mandarin cv. ‘Clemenules’. *Radiation Physics and Chemistry*, 76, 1631 – 1635.
- Ay, M. R., & Zaidi, H. (2006). Assessment of errors caused by X-ray scatter and use of contrast medium when using CT-based attenuation correlation in PET. *European Journal of Nuclear Medicine and Molecular Imaging*, 33, 1301 – 1313.
- Barreiro, P., Zheng, C., Sun, D, Hernández-Sánchez, N., Pérez-Sánchez, J. M., & Ruiz-Cabello, J. (2008). Non-destructive seed detection in mandarins: Comparison of automatic threshold methods in FLASH and COMSPIRA MRIs. *Postharvest Biology and Technology*, 47, 189-198.
- Bobelyn, E., Serban, A., Nicu, M., Lammertyn, J., Nicolai, B. M., & Saeys, W. (2010). Postharvest quality of apple predicted by NIR-spectroscopy: Study of the effect of biological variability on spectra and model performance. *Postharvest Biology and Technology*, 55, 133-143.
- Cantre, D., Herremans, E., Verboven, P., Ampofo-Asiama, J., Nicolai, B. (2014). Characterization of the 3-D microstructure of mango (*Mangifera indica* L. cv. Carabao) during ripening using X-ray computed microtomography. *Innovative Food Science and Emerging Technologies*, 24, 28 – 39.
- Cayuela, J. A. (2008). Vis/NIR soluble solids prediction in intact oranges (*Citrus sinensis* L.) cv. Valencia Late by reflectance. *Postharvest Biology and Technology*, 47, 75 – 80.
- Cayuela, J. A., & Weiland, C. (2010). Intact orange quality with two portable NIR spectrometers. *Postharvest Biology and Technology*, 58, 113 – 120.

- Chen, Q., Zhang, C., Zhao, J., & Ouyang, Q. (2013). Recent advances in emerging imaging techniques for non-destructive detection of food quality and safety. *Trends in Analytical Chemistry*, 52, 261 – 274.
- Chuang, C., Ouyang, C., Lin, T., Yang, M., Yang, E., Huang, T., Kuei, C., Luke, A., & Jiang, J. (2011). Automatic X-ray quarantine scanner and pest infestation detector for agricultural products, *Computers and Electronics in Agriculture*, 77, 41-59.
- Cozzolino, D., Cynkar, W. U., & Smith, P. (2011). Multivariate data analysis applied to spectroscopy: potential application to juice and fruit quality. *Food Research International*, 44, 1888 – 1896.
- Department of Agriculture, Forestry and Fisheries (DAFF). (2012). Regulations relating to the grading, packing and marking of citrus fruit intended for sale in the Republic of South Africa. http://www.gov.za/sites/www.gov.za/files/35910_9864_gon963.pdf (last accessed 29.09.2015).
- Department of Agriculture, Forestry and Fisheries (DAFF). (2016). Agricultural product standards act, 1990 (Act No. 119 of 1990) standards and requirements regarding control of the export of citrus fruit. <http://www.daff.gov.za/daffweb3/Branches/Agricultural-Production-Health-Food-Safety/Food-Safety-Quality-Assurance/Export-Standards/Citrus-and-Subtropical-Fruit/Citrus-fruit> (last accessed 11.02.2017).
- Fraser, D. G., Jordan, R. B., Kunemeyer, R., & McGlone, V. A. (2003). Light distribution inside mandarin fruit during internal quality assessment by NIR spectroscopy. *Postharvest Biology and Technology*, 27, 185-196.
- Friebel, M., Kroh, L. W., Lurie, S., Meinke, M., Rohn, S., & Torricelli. (2009). What to measure and how to measure. In: *Optic Monitoring of Fresh and Processed Agricultural Crops*, Taylor & Francis Group, Florida, USA.
- Goldman, L. W. (2007). Principles of CT: Radiation Dose and Image Quality. *Journal of Nuclear Medicine Technology*, 35, 213 – 225.
- Gomez, A.H., He, Y., & Pereira, A.G. (2006). Non-destructive measurement of acidity, soluble solids and firmness of Satsuma mandarin using Vis-NIR spectroscopy techniques. *Journal of Food Engineering* 77, 313 - 319.

- Guthrie, J. A., Walsh, K. B., Reid, D. J., & Liebenberg, C. J. (2005a). Assessment of internal quality attribute of mandarin fruit. 1. NIR calibration model development. *Australian Journal of Agricultural Research*, 56, 405-416.
- Guthrie, J. A., Reid, D. J., & Walsh, K. B. (2005b). Assessment of internal quality attribute of mandarin fruit. 2. NIR calibration model robustness. *Australian Journal of Agricultural Research*, 56, 417 – 426.
- Haff, R. P., & Pearson, T. C. (2007). An automatic algorithm for detection of infestations in X-ray images of agricultural products. *Sensing and Instrumentation for Food Quality and Safety*, 1, 143–150.
- Hernandez-Sanchez, N., Barreiro, P., & Ruiz-Cabello, J. (2006). On-line Identification of Seeds in Mandarins with Magnetic Resonance Imaging, *Biosystems Engineering*, 95, 529-536.
- Herremans, E., Verboven, P., Bongaers, E., Estrade, P., Verlinden, B. E., Wevers, M., Hertog, M. L. A. T. M., & Nicolai, B. M. (2013). Characterization of ‘Braeburn’ browning disorder by means of X-ray micro-CT. *Postharvest Biology and Technology*, 75, 114 – 124.
- Herremans, E., Melado-Herreros, A., Defraeya, T., Verlinden, B., Hertog, M., Verboven, P., Val, J., Fernandez-Valle, M. E., Bongaers, E., Estrade, P., Wevers, M., Barreiro, P., & Nicolai, B. M. (2014a). Comparison of X-ray CT and MRI of watercore disorder of different apple cultivars. *Postharvest Biology and Technology*, 87, 42 – 50.
- Herremans, E., Verboven, P., Defraeye, T., Rogge, S., Ho, Q. T., Hertog, M. L. A. T. M., Verlinden, B. E., Bongaers, E., Wevers, M. & Nicolai, B. M. (2014b). X-ray CT for quantitative food microstructure engineering: The apple case, *Nuclear Instruments and Methods in Physics Research B*, 324, 88-94.
- Huang, H., Yu, H., Xu, H., & Ying, Y. (2008). Near infrared spectroscopy for on/in-line monitoring of quality in foods and beverages: A review. *Journal of Food Engineering*, 87, 303–313

- Jamshidi, B., Minaei, S., Mohajerani, E., & Ghassemian, H. (2012). Reflectance Vis/NIR spectroscopy for non-destructive taste characterization of Valencia oranges. *Computers and Electronics in Agriculture*, 85, 64 – 69.
- Jha, S. N., & Matsuoka, T. (2000). Non-destructive techniques for quality evaluation of intact fruits and vegetables. *Food Science Technology*, 6, 248-251.
- Jiang, J. A., Changa, H. Y., Wu K. H, Ouyang, C. S., Yang, M. M, Yang, E. C., Chen, T. W., and Lin, T.T. (2008). An adaptive image segmentation algorithm for X-ray quarantine inspection of selected fruits. *Computers and Electronics in Agriculture*, 60, 190 - 200.
- Kotwaliwale, N., Singh, K., Kalne, A., Jha, S. N., Seth, N., et al. (2014). X-ray imaging methods for international quality evaluation of agricultural produce. *Journal of Food Science and Technology*, 51, 1-15.
- Ladaniya, M. S. (2008). Citrus fruit: Biology, technology and evaluation, Elsevier Inc., London, UK.
- Lammertyn, J., Peirs, A., De Baedemaeker, J., & Nicolai, B. (2000). Light penetration properties of NIR radiation in fruit with respect to non-destructive quality assessment. *Postharvest Biology and Technology*, 18, 121-132.
- Lammertyn, J., Dresselaers, T., Van Hecke, P., Jancsok, P., Wevers, M., et al. (2003a). Analysis of time course of core breakdown in ‘Conference’ pears by means of MRI and X-ray CT. *Postharvest Biology and Technology*, 29, 19 - 28
- Lammertyn, J., Dresselaers, T., Van Hecke, P., Jancsok, P., Wevers, M., et al. (2003b). MRI and X-ray CT study of spatial distribution of core breakdown in ‘Conference’ pears. *Magnetic Resonance Imaging*, 21, 805 - 815.
- Li, J., Huang, W., Tian, X., Wang, C., Fan, S., & Zhao, C. (2016). Fast detection and visualization of early decay in citrus using Vis-NIR hyperspectral imaging. *Computers and Electronics in Agriculture*, 127, 582 – 592.
- Liu, Y., Sun, X., Zhang, H., & Aiguo, O. (2010). Nondestructive measurement of internal quality of Nanfeng mandarin fruit by charge coupled device near infrared spectroscopy. *Computers and Electronics in Agriculture*, 71S, S10 –S14.

- Lin, T., Jiang, J., Ouyang, C., & Chang, H. (2005). Intergration of an automatic X-ray scanning system for fruit quarantine. International Conference on Automation Technology. (May 5 to 6).
- Louw, E. D., & Theron, K. I. (2010). Robust prediction models for quality parameters in Japanese plums (*Prunus salicina* L.) using NIR spectroscopy, *Postharvest Biology and Technology*, 58, 176 – 184.
- Lu, R. (2008). Quality evaluation of Fruit by Hyperspectral Imaging. In: Computer Vision Technology for Food Quality Evaluation, Elsevier Inc, East Lansing , USA.
- Mabood, F., Al-Harrasi, A., Boqué, R., Jabeen, F., Hussain, J., Hafidh, A., Hind, K., Ahmed, M.A.G., Manzoor, A., Hussain, H., Rehman, N. U., Iman, S.H., Said, J. J., Hamood, S. A. (2015). Determination of sucrose in date fruits (*Phoenix dactylifera* L.) growing in the Sultanate of Oman by NIR spectroscopy and multivariate calibration. *Spectrochimica Acta Part A: Molecular and Biomolecular Spectroscopy*, 150, 170 - 174.
- Magwaza, L. S., Opara, U. L., Nieuwoudt, H., Cronje, P. J. R., Saeys, W., & Nicolai, B. (2012). NIR Spectroscopy Applications for Internal and External Quality Analysis of Citrus Fruit—A Review, *Food Bioprocess Technology*, 5, 425–444.
- Magwaza, L. S., Ford, H. D., Cronje, P. J. R., Oparaa, U. L., Landahl, S., Tatam, R. P., & Terry, L. A. (2013). Application of optical coherence tomography to non-destructively characterize rind breakdown disorder of ‘Nules Clementine’ mandarins. *Postharvest Biology and Technology*, 84, 16-21.
- Magwaza, L. S., Opara, U. L., Cronje, P. J. R., Landahl, S., Nieuwoudt, H. H., Mouazen, A. M., Nicolai, B. M., & Terry, L. A. (2014a). Assessment of rind quality of ‘Nules Clementine’ mandarin during postharvest storage: 1. Vis/NIRS PCA models and relationship with canopy position. *Scientia Horticulturae*, 165, 410 – 420.
- Magwaza, L. S., Opara, U. L., Cronje, P. J. R., Landahl, S., Nieuwoudt, H. H., Mouazen, A. M., Nicolai, B. M., & Terry, L. A. (2014b). Assessment of rind quality of ‘NulesClementine’ mandarin fruit during postharvest storage: 2. Robust Vis/NIRS PLS models for prediction of physico-chemical attributes. *Scientia Horticulturae*, 165, 421 – 432.

- Magwaza, L. S., & Opara, U. L. (2014). Investigating non-destructive quantification and characterization of pomegranate fruit internal structure using X-ray computed tomography. *Postharvest Biology and Technology*, 95, 1 – 6.
- McGlone, A. V., Fraser, D. G., Jordan, R. B., & Kunemeyer, R. (2003). Internal quality assessment of mandarin fruit by vis/NIR spectroscopy. *Near Infrared spectroscopy*, 11, 323 – 332.
- Miller, J. N., & Miller, J. C. (2010). *Statistics and Chemometrics for Analytical Chemistry*. Pearson Education Limited, England, UK.
- Musse, M., Quellec, S., Devaux, M. F., Cambert, M., Lahaye, M., & Mariette, F. (2009). An investigation of the structural aspects of the tomato fruit by means of quantitative nuclear magnetic resonance imaging. *Magnetic Resonance Imaging*, 27, 709 – 719.
- Ncama, K., Opara, U. L., Tesfay, S. Z., Fawole, O. A., & Magwaza, L. S. (2017). Application of Vis/NIR spectroscopy for predicting sweetness and flavour parameters of ‘Valencia’ orange (*Citrus sinensis*) and ‘Star Ruby’ grapefruit (*Citrus x paradisi* Macfad). *Journal of Food Engineering*, 193, 86 – 94
- Nicolai, B. M., Beullens, K., Bobelyn, E., Peirs, A., Saeys, W., Theron, K. I., & Lammertyn, J. (2007). Nondestructive measurement of fruit and vegetable quality by means of NIR spectroscopy: A review. *Postharvest Biology and Technology*, 46, 99 – 118.
- Nicolai, B. M., Bulens, I., Josse De Baerdemaeker, DeKetelaere, B., Hertog, M. L.A.T. M., Verboven, P., and Lammertyn, J. (2009). Non-destructive evaluation: Detection of external and internal attributes frequently associated with quality and damage. In: *Postharvest Handling: A Systems Approach*, Elsevier, London, UK.
- Nicolai, B. M., Defraeye, T., De Ketelaere, B, Herremans, E., Hertog, M. L. A. T. M., Saeys, W., Torricelli, A., Vandendriessche, T., & Verboven, P. (2014). Nondestructive measurement of fruit and vegetable quality. *Annual Review Food Science Technology*, 5, 285 – 312.
- Ogawa, Y., Kondo, N., & Shibusawa, S. (2003). Inside quality evaluation of fruit by X-ray image. Proceedings of the 2003 IEEUASME International Conference on Advanced Intelligent Mechatronics

- Omar A. F. B. & MatJafri M. Z. B. (2009). Optical sensor in the measurement of fruits quality:A review on an innovative approach. *International Journal of Computer and Electrical Engineering*, 1, 1793 – 8163.
- Peiris, K. H. S., Dull, G. G., & R. G. Leffler. (1998). Nondestructive detection of section drying, an internal disorder in tangerine. *HortScience*, 33, 310 – 312.
- Peirs, A., Scheerlinck, N., & Nicolai, B. M. (2003). Temperature compensation for near infrared reflectance measurement of apple fruit soluble solids contents. *Postharvest Biology and Technology*, 30, 233 – 248.
- Perez-Marin, D., Paz, P., Guerrero, J., Garrido-Varo, A., & Sanchez, M. (2010). Miniature handheld NIR sensor for the on-site non-destructive assessment of post-harvest quality and refrigerated storage behavior in plums, *Journal of Food Engineering*, 99, 294 – 302.
- Rungpichayapichet, P., Mahayothee, B., Nagle, M., Khuwijitjaru, P., & Muller, J. (2016). Robust NIRS models for non-destructive prediction of postharvest fruit ripeness and quality in mango. *Postharvest Biology and Technology*, 111, 31 – 40.
- Sanchez, M. T., De la Haba, M. J. & Perez-Marin, D. (2013). Internal and external quality assessment of mandarins on-tree and at harvest using a portable NIR spectrophotometer. *Computers and Electronics in Agriculture*, 92, 66-74.
- Schwanninger, M., Rodrigues, J. C., & Fackler, K. (2011). A review of band assignments in near infrared spectra of wood and wood components. *Journal of Near Infrared Spectroscopy*, 19, 287 – 308.
- van Dael, M., Lebotsa, S., Herremans, E., Verboven, P., Sijbers, J., Opara, U. L., Cronje, J., & Nicolai, B. (2016). A segmentation and classification algorithm for online detection of internal disorders in citrus using X-ray radiographs, *Postharvest Biology and Technology*, 112, 205-214.
- Walsh, K. B. (2005). Commercial adoption of technologies for fruit grading, with emphasis on NIRS. *Information and Technology for Sustainable Fruit and Vegetable Production*, 5, 399 – 404.

Wang, A., Hu, D., & Xie, L. (2014). Comparison of detection modes in terms of the necessity of visible region (VIS) and influence of the peel on soluble solid content (SSC) determination of navel orange using VIS-SWNIR spectroscopy. *Journal of Food Engineering*, 126, 126-132.

Xudong, S., Hailiang, Z. & Yande, L. (2009). Nondestructive assessment of quality of Nafeng mandarin fruit by a portable near infrared spectroscopy. *International Journal of Agricultural and Biological Engineering*, 2, 1, 65 – 71.

3. Detection of granulation in ‘Navel’ orange and ‘Nadorcott’ mandarin seeds using X-ray computed tomography

Abstract

The presence of granulation in ‘Navel’ orange and seeds in ‘Nadorcott’ mandarin are some of the major quality issues affecting citrus fruit. Affected fruit does not show visible external symptoms and are therefore difficult to detect and sort. The aim of this study was to investigate the detection of granulation in ‘Navel’ orange and seeds in ‘Nadorcott’ mandarin based on radiographic and tomographic images. Both tomographic and radiographic images were able to reveal the presence of granulation in ‘Navel’ orange fruit. Classification of granulated ‘Navel’ orange fruit based on tomographic images yielded better results (86%) than radiographic images (70%). On seeds detection, radiographic images were unable to reveal seeds in ‘Nadorcott’ fruit. This was contrary to the application of tomographic images as they were able to reveal ‘Nadorcott’ seeds despite its inability to clearly separate the seeds from the endocarp of the fruit. The use of radiographic and tomographic images can therefore, be useful in the detection of granulation disorder for classification purposes.

3.1 Introduction

Citrus is an important crop in the international trade due partly to its health benefits (Vicente et al., 2009; Zou et al., 2016). The citrus industry is, however, faced with challenges such as fruit physiological disorders and defects which affect fruit quality and market value (Sharma et al., 2006; Ladaniya, 2008; Kotwaliwale et al., 2014). The disorders include fruit splitting or cracking, rind pitting, sunburn, freeze injury, chilling injury, granulation, rind staining and rind breakdown (Ladaniya, 2008). Disorders such as granulation have little or no visible external symptoms. Much more, the presence of internal disorders without external visual symptoms make it difficult to detect affected fruit which in turn poses considerable threats in export marketing due to potential claims and reject of affected shipment (Lammertyn et al., 2003).

While several of citrus fruit disorders remain paramount, granulation disorder, which ultimately has no visible external symptoms, poses industrial problems during postharvest sorting at the packing house (Ritenour, 2004; Sharma et al., 2006; Zhang et al., 2016).

Granulation is a physiological disorder wherein juice sacs become hard and dry, resulting in reduced extractable juice in citrus fruit (Ritenour, 2004; Sharma & Saxena, 2004; Ladaniya, 2008). This disorder has been reported in mandarins, grapefruit and oranges (Peiris et al., 1998; Ritenour, 2004). The factors reported to influence the development of granulated disorder in fruit are mainly pre-harvest factors and these include cultivar, delayed harvest, crop load and fruit size, orchard location and climate, as well as irrigation and fertilizer application practices (Peiris et al., 1998; Ritenour, 2004). Among several detection methods adopted to evaluate fruit with disorders, the non destructive detection techniques have been of greater importance to fruit industry (Peiris et al., 1998).

In addition to fruit disorders, seeds in certain citrus cultivars are known to affect fruit quality and market value (Chao, 2005; JingPing et al., 2009). As reported in several scientific studies, consumer acceptance of citrus fruit has been shown to be influenced by presence of seeds (Raza et al., 2003; Hernandez-Sanchez et al., 2006; JinPing et al., 2009). For instance, Chao (2005) reported an increase in preference of seedless citrus fruit as opposed to citrus fruit with seeds. The breeding of citrus fruit among different cultivars can either result in seedless or seedy citrus fruit (Chao, 2005). For example, ‘Nadorcott’ mandarin, one of the most popular soft citrus cultivars in South Africa is seedless when self-pollinated but get seedy when cross pollinated with other cultivars (Chao, 2005; Sikuka, 2015). As an implication, it is important therefore to detect and quantify seeds in citrus fruit for the purpose of sorting and processing.

Various imaging techniques used for assessment of fruit internal structure have been reviewed in literature (Chen et al., 2013; Nicolai et al., 2014). Among those techniques, X-ray computed tomography (X-ray CT) has been reported to have a capability of obtaining high resolution images of internal structures of plant material (Nicolai et al., 2009). Also, the large field of view of X-ray CT allows for whole fruit analysis (Lammertyn et al., 2003; Gueven & Hicsasmaz, 2013). The technique is a well-established non-destructive detection method used for the evaluation of internal defects in fruit. X-ray CT has been successfully applied in agricultural and food industries for inspection purposes (Jha & Matsuoka, 2000).

The extensive application of X-ray CT on fruits such as guava, peaches, pears, apples and citrus for detection of internal disorders as well as presence of alien materials has been reported in literature (Barcelon et al., 1999; Lammertyn et al., 2003; Half & Toyofuku, 2008). Existing researches include detection of internal disorders in citrus (Peiris et al., 1998; van

Dael et al., 2016), and investigations of pests infested injuries, core breakdown, browning disorder, watercore disorder; variations during ripening as well as quantification of volumes fruit fractions in other fruits (Lammertyn et al., 2003; Lin et al., 2005; Jiang et al., 2008; Haff & Pearson, 2007; Chuang et al., 2011; Herremans et al., 2013; Herremans et al., 2014a; Herremans et al., 2014b; Magwaza & Opara, 2014; Arendse et al., 2016; Cantre et al., 2014).

Although X-ray CT has been applied in ‘Navel’ oranges, quantification of extent of granulation has only been studied based on radiographic images (van Dael et al., 2016). While X-ray radiographs were able to detect endoxerosis in ‘Eureka’ lemon and granulation in ‘Navel’ orange, van Dael et al. (2016) reported that detection to a large extent could be achieved using tomographic images. Radiographic images contain cumulative data which do not reveal the gradual change in grey value of fruit while tomographic images are three dimensional (3D), allowing characterization of physical and physiological structures of biological materials (Opara & Magwaza, 2014; van Dael et al., 2016).

This study therefore aims to investigate the detection of granulation in ‘Navel’ orange based on both radiographic and tomographic images. Regarding seeds detection, researchers have investigated the presence of seeds in citrus (mandarins and oranges) using magnetic resonance imaging (MRI) (Hernandez et al., 2005; Hernandez-Sanchez et al., 2006; Barreiro et al., 2008). However, little is known about the prospects of detecting the presence of seeds in ‘Nardacott’ mandarins using X-ray CT. Therefore, the present study aims to investigate detection of seeds in ‘Nardacott’ mandarin based on X-ray CT radiographic and tomographic images.

3.2 Materials and methods

3.2.1 Citrus fruit

‘Nardacott’ mandarin fruit and ‘Navel’ orange fruit were harvested from a commercial orchard in Marble Hall, Mpumalanga, South Africa (25°06'16.57" S, 29°25'50.65" E). Fruits were harvested in August 2011, packed in cartoon and transported from South Africa to Belgium via air freight. Samples were limited to 30 ‘Navel’ orange fruit and 30 ‘Nadorcott’ mandarin fruit. On arrival, the samples were stored at a temperature of 4 °C, at KU Leuven, Belgium, until imaging experiment.

3.2.2 X-ray computed tomography

Fruits were removed from 4°C storage and allowed to reach room temperature before measurements were taken. Fruits were scanned on an X-ray Computed Tomography (AEA Tomohawk, Philips) at the Department of Materials Engineering, KU Leuven, Belgium. Each was positioned on the rotating table with the stylar-end to stem end-axis of the fruit parallel with the scanner axis of rotation (Figure 3.1). The scanner was operated at a source voltage of 75 kV, current of 468 mA, with pixel sizes of 77.6 μm and 128.9 μm for mandarins and oranges respectively, with exposure time of 60 ms. For each fruit, radiographic projections of 1024 by 1024 pixels at angular steps of 0.3° were obtained.

To validate results computed from X-ray CT image analysis, fruits were destructively evaluated for the presence of granulation and seeds immediately after X-ray imaging. In order to evaluate granulation, ‘Navel’ oranges were sliced at ± 15 mm intervals to observe the presence of granulation disorder. To evaluate presence of seeds, ‘Nardacott’ mandarins were cut open to count the seeds contained in all the samples.



Figure 3.1 X-ray equipment showing position of fruit during scanning.

3.2.3 Image processing

Radiographic images were analysed using ImageJ software. Tomographic (3D) images were constructed from radiographic images using NRecon 1.6.2.0 (Bruker microCT, Kontich, Belgium). This resulted in stacks of grey scale images (Figure 3.2a). The resulting reconstructed 3D image had a size of 1024 x 1024 x 1024 with each isotropic voxel measuring 128.9 and 99.6 μm^3 for mandarins and oranges respectively. Analysis of the tomographic images was performed using VGStudioMax version 2.2. Before analyses, every

image was pre-processed by removing the background to be able to analyse only orange tissue (the Volume of Interest, VOI).

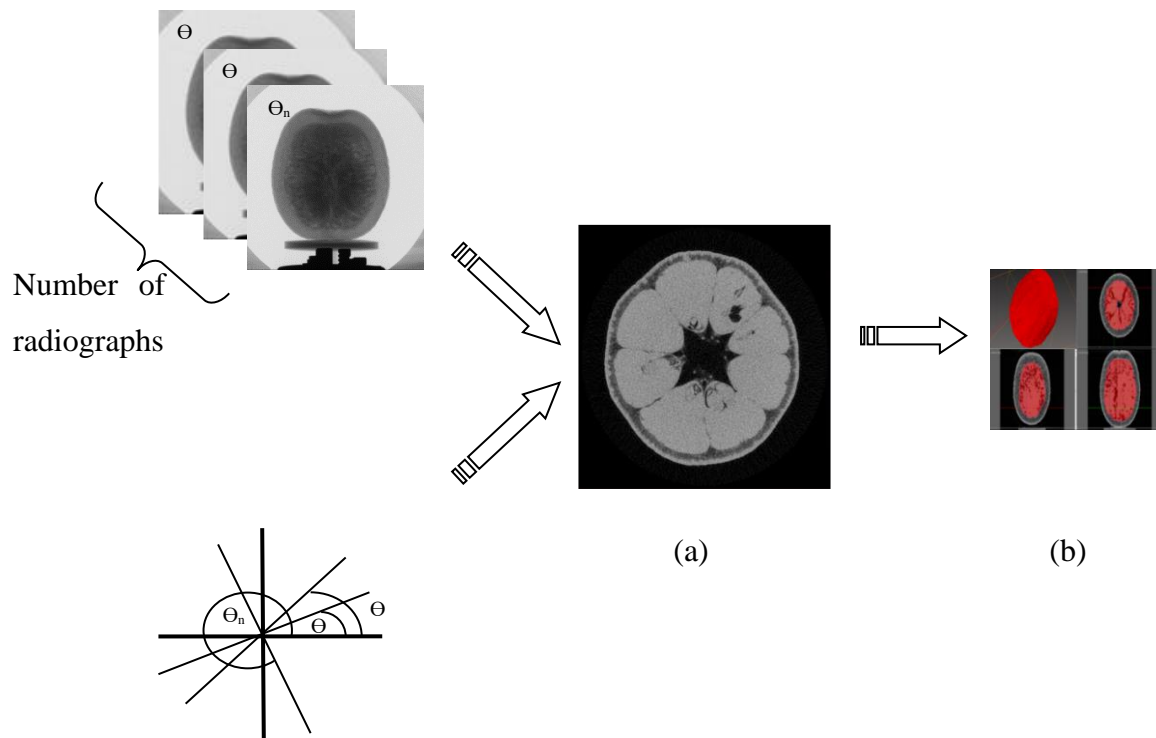


Figure 3.2 Conversion of radiographic images to tomographic images, slice of tomographic image reconstructed from NRecon (a) and 3D image (b).

3.2.4 Feature extraction

Radiographs were processed individually to identify area of granulation. Two distinct areas regions were observed, the unaffected tissue (low pixel intensity) and the combined region of exocarp, mesocarp and affected endocarp (high pixel intensity). The radiographic images were processed using ImageJ, following method used by van Dael et al. (2016) modified. Otsu thresholding method was applied. The first threshold separated the entire fruit from the background. The second threshold separated the unaffected tissue from combined region of exocarp, mesocarp and affected endocarp. These thresholds were determined for the radiographic images of unaffected samples, after which the mean of these values was used for segmentation of all the images. Once the radiographic images were segmented, properties or features (Table 3.1), of the regions representing the unaffected endocarp were calculated.

Table 3.1 Features of regions representing unaffected endocarp from radiographic images of ‘Navel’ oranges

Feature	Description
Total perimeter (pixels)	Perimeter of the unaffected endocarp.
Area/perimeter (pixels)	Ratio of the total area unaffected endocarp to the total perimeter of unaffected endocarp.
Solidity (%)	Ratio of the area of unaffected endocarp to the area of the convex hull of the region.

3.2.5 Histogram analysis

The histograms of the 3D images were analysed using Microsoft Excel to study the differences in grey level distribution between healthy and granulated oranges. The histograms were analysed using the method used by Herremans et al. (2014b) with modification. The background was removed to be able to analyse only orange tissue (VOI). The statistical features, variance, skewness and kurtosis of these grey level histograms of each image were computed. Analysis of Variance (ANOVA) was performed to identify statistically significant difference ($p < 0.05$) between the images of the healthy and of granulated fruit.

3.2.6 3D microstructural analysis

The X-ray CT images were analysed in 3D in order to compare and quantify the microstructure of healthy and granulated fruit. Microstructure was analysed using the method used by Herremans et al. (2013) and du Plessis et al. (2014) with modifications. Reconstructed volumes were analysed with VGStudioMax 2.2 with defect analysis module. The data was smoothed using a median filter before the analysis, to remove noise. The background was removed to be able to analyse only orange tissue (VOI). Once the VOI was created, an automated defect analysis was done using the defect analysis module. This function generates information on each individual pore including diameter, volume, surface area and sphericity. The information enabled computation of the morphometric parameters of the microstructures and are summarised in Table 3.2.

Table 3.2 Description of 3-D morphometric parameters used to quantify the microstructure of apple tissue

Microstructural parameter	Description
Volume (cm ³)	Volume of the object
Area (cm ²)	Area of the object
Specific surface area (cm ⁻¹)	Area divided by the volume of the object
Porosity (%)	Pore volume divided by total volume of analysed tissue
Skewness	Skewness of individual pore volume distribution
Kurtosis	Kurtosis of individual pore volume distribution

3.2.7 Classification

In the classification stage of radiographic images, features described previously were calculated in each image. Multivariate discriminant analysis was applied on the set of data to investigate the classification of granulated and non-granulated ‘Navel’ orange fruit based of the calculated features. For the 3D images, the morphometric parameters described in Table 2 were calculated for each fruit. Multivariate discriminant analysis was also applied on the 3D data to investigate classification of granulated and non-granulated based on the 3D morphometric parameters. Classification accuracies were extracted for each set of data, which show the proportion of correctly classified data into the two categories (granulated and non-granulated).

3.3 Results and discussion

3.3.1 Radiographic and tomographic images

Figure 3.3 shows radiographic and digital photographs of granulated and healthy ‘Navel’ orange fruit. Based on the observed granulation on the radiographic images (Figure 3.3b), the disorder can be seen as regions of higher intensity. The presence of granulation was observed at the stem-end and the styler-end of the fruit; however, on severely affected fruit, it was shown to spread throughout the entire fruit (Figure 3.3b). This is consistent with the findings of van Dael et al. (2016) who reported similar results in lemon and granulated oranges affected by endoxerosis. Interestingly, the images derived for granulated and non-granulated ‘Navel’ oranges using digital and X-ray techniques were strikingly similar (Figure 3.3).

Nielsen et al. (2014) reported slight variation in contrast on radiographic images between fresh and frozen or defrosted blackberry, blueberry and mandarin fruit pieces. Nielson et al. (2014) reported that even though the microstructure in the berries changes dramatically when being frozen or defrosted, the X-ray radiographs are not sensitive to the X-ray scattering originating from the microstructure of the sample, but are rather sensitive to changes in density hence the variation was minimal. Due to the sensitivity of X-ray attenuation to density, higher contrast in the current study may be attributed to a reduction in density in granulated regions. Furthermore, there were no observable differences between radiographic images of seeded and non-seeded ‘Nadorcott’ mandarins as these images did not reveal the presence of seeds in the fruit.

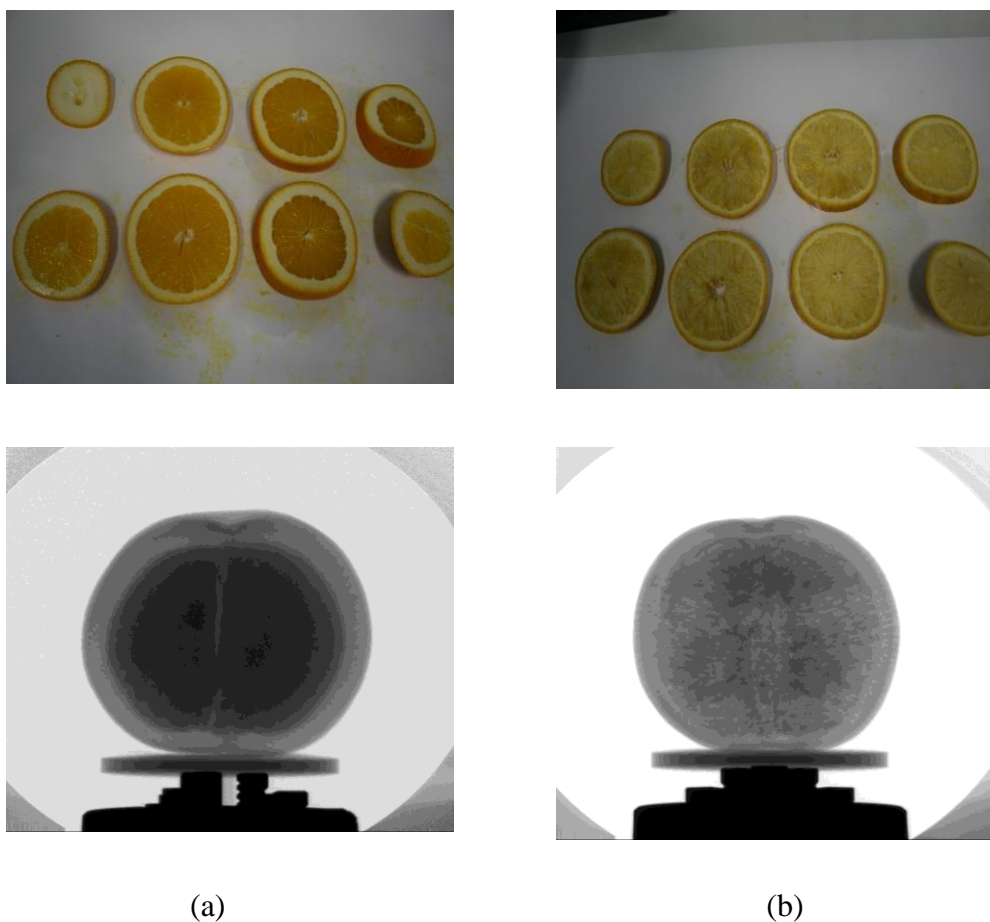


Figure 3.3 Radiographic and digital images of a healthy ‘Navel’ orange (a) and a granulated fruit (b) with corresponding digital images (top).

In contrast to radiographic images, tomographic images revealed granulation of ‘Navel’ orange as darker regions (lower intensity). Again, the tomographic images were much identical to that of digital images of ‘Navel’ oranges (Figure 3.4a). In agreement with literature findings, section drying on tangerine was reported to appear as darker areas in X-ray images (Peiris et al., 1998). Also, van Dael et al. (2016) recounted similar details as they saw fruit disorder appeared on tomographic images as regions of lower intensity. This was attributed to the absorption of X-ray in that region since X-ray is dependent on fruit tissue’s water content and density. As a consequence, a fruit tissue with a low density normally results in a low X-ray absorption hence darker imaging (Peiris et al., 1998).

In peach, the inner portion showed dark regions after two weeks of ripening. This was attributed to the minimal absorption of X-ray in those regions as the regions became drier and developed voids (Barcelon et al., 1999). Lammertyn et al. (2003) studied the core breakdown

in pears and observed lower intensity areas indicating lower density in regions where browning occurred. Also, Herremans et al. (2014a) reported that dehydrated tissues in apples were marked by lower intensities when benchmarked against surrounding tissues. A similar trend in microtomographic images of kiwifruit was found by Cantre et al. (2014) as they recounted lightness in association with denser cells and vice versa in low density pores.

On the other hand, the presence of seeds in ‘Nadorcott’ mandarin appeared as a group of pixels surrounded by lower intensity boundary found towards the central axis of the fruit (Figure 3.4b). However, the pixels within the boundary had similar intensity as the pixels of the fruit flesh. The similarity in pixel intensity indicated that the densities of both the tissue and the seeds were equal. This was, however, contrary to the findings reported by Barreiro et al. (2008) as they presented magnetic resonance imaging (MRI) to clearly show distinct differences between the flesh and seeds of mandarin. In addition, the authors reported the seeds to be characterised by increase in lower intensity region and morphological distortions (Barreiro et al., 2008).

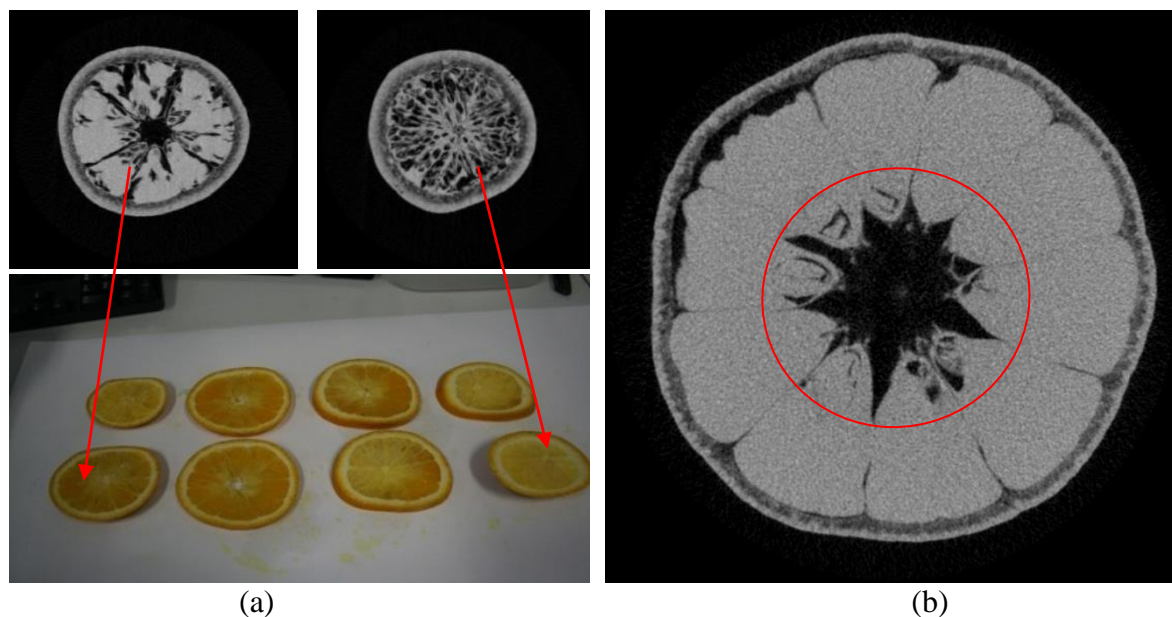


Figure 3.4 Tomographic images of granulated ‘Navel’ orange (a) and ‘Nadorcott’ mandarin with seeds (b)

3.3.2 Features of radiographic

3.3.2.1 Quantitative parameters of disorder

Table 3.3 shows the mean feature values with standard deviations derived from the images used for classification as well as unprocessed and segmented images of granulated and non-granulated ‘Navel’ orange. The solidity and ratio of area to perimeter increased with affected fruit while perimeter decreased with affected fruit. Similar results were observed in granulated ‘Navel’ orange fruit and in ‘Eureka’ lemon fruit affected by endoxerosis using X-ray radiographic images by van Dael et al. (2016). The author suggested that the increase in perimeter affected fruit may be due to the segmented area being broken into regions (Table 3.3). The ratio of area to perimeter decreased with affected fruit due to an increase in perimeter. Solidity (ratio of the area of unaffected endocarp to the area of the convex hull of the region) decreased with affected fruit due in a decrease in area.

Table 3.3 Mean and standard deviation for parameters of radiographs with and without granulation disorder, used as feature values for classification of ‘Navel’ oranges.

	Healthy fruit	Granulated fruit
Unprocessed images		
Segmented unaffected tissue		
N	9	21
Area (pixels)	600871.80±35.18	7598.77±20.67
Perimeter (pixels)	1575.05±74.	3178.19±96.08
Area/perimeter	11.63±1.73	10,91± 0.82
Solidity	0.54 ±0.16	0.44±0.12

3.3.2.2 Classification based on radiographic images

The statistics indicated that the discriminant analysis could distinguish between granulated tissue and healthy tissue of ‘Navel’ orange based on radiographic images. By that, 21 (70%) out of 30 samples were correctly classified into granulated and non-granulated groups (Table 3.4). Van Dael et al. (2016) correctly classified 93.9% oranges and 92.8% lemons on X-ray radiographic images, when using validated k-nearest neighbours (kNN) classifiers. Hernandez-Sanchez et al. (2006) obtained a correct classification of 88.9% for seeded and 86.7% for non-seeded mandarins when using discriminant analysis on MRI coronal images. Barreiro et al., (2008) obtained correct classification of 94.5% and 73.9% for seedless and seed-containing mandarins respectively, when using discriminant analysis on MRI coronal images.

Table 3.4 Classification results for classification of ‘Navel’ orange fruit according to granulated and non-granulated based on radiographic image features.

	Class	Number	Correct	Granulated	Non-granulated
Class	Granulated	21	66.67%	16	7
	Non-granulated	9	55.55%	4	5

Classification success: 70%

3.3.3 Tomographic images

3.3.3.1 Histogram analysis

Histograms of granulated and non-granulated ‘Navel’ oranges are shown in Fig. 5. The histogram of a healthy ‘Navel’ orange and that of a granulated ‘Navel’ orange are both bimodal. The tomographic image of granulated fruit has more pixels with lower intensity than that of a healthy fruit. The patterns deduced according to the present research were contrary to that observed for apple with watercore by Herremans et al. (2014b), where the histogram of disordered fruit had more pixels with high grey value. X-ray attenuation depends on density of material (Peiris et al., 1998) and therefore the difference can be associated to the reduced density in granulated tissue of ‘Navel’ orange and increased density with watercore affected tissue of apple.

Magwaza & Opara (2014) observed a similar trend for pomegranate fruit but with three peaks with the variation being brought about by air spaces in the fruit. Cantre et al. (2014) on the

other hand observed unimodal histograms in X-ray CT images of ripe and of unripe mango fruit. The author further explained that the lack of clear separation in peaks was due to small pore space which appeared at the front tail of the histogram without any clear separation between the pore and tissue peak.

Table 3.5 shows the variance, skewness and kurtosis derived for both healthy and granulated orange fruit. Based on statistical analysis, no significant differences in skewness and kurtosis between the healthy and the granulated fruit were obtained. This was contrary to the variance of healthy and granulated fruit. A significant difference between the variance of the histograms of granulated and non-granulated fruit was reported (Table 3.5). This confirms the difference in pixel intensity distribution between the healthy and the granulated fruit observed in the histograms (Figure 3.5). The results are similar to those observed for apple by Herremans et al. (2014b), where the variance in was significantly different between watercore apples and healthy apples. This was in agreement with the general conclusions of Herremans et al. (2014b). The information generated from the histograms revealed the practical implications of using X-ray computed tomography to distinguish between granulated and non-granulated fruit.

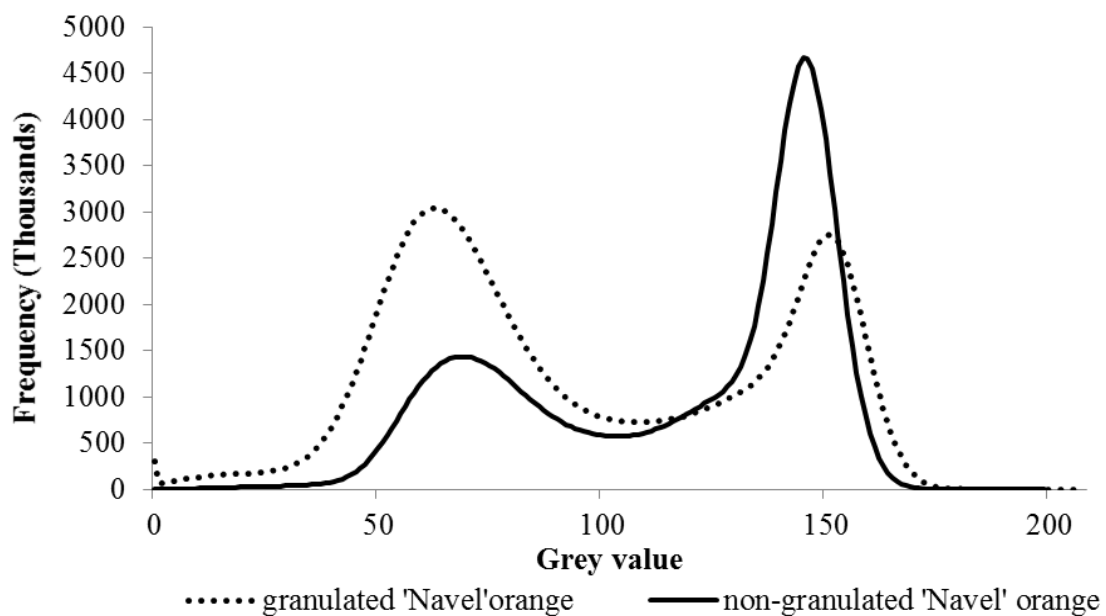


Figure 3.5 Distribution of grey values for radiographic images (8-bit grey scale) of a granulated and a non-granulated 'Navel' orange fruit.

Table 3.5 Range, mean and standard deviation (SD) for the histograms of granulated (n = 9) and non-granulated fruit, healthy (n=9), granulated (n = 21).

	Health fruit	Granulated fruit
Variance	$1.86 \times 10^9 \pm 2.71 \times 10^{8a}$	$1.54 \times 10^9 \pm 2.59 \times 10^{8b}$
Skewness	15.92 ± 0.04^a	15.89 ± 0.05^a
Kurtosis	254.39 ± 0.88^a	253.62 ± 1.18^a

Means in the same row with different letter(s) differ significantly ($p \leq 0.05$).

3.3.3.2 Quantitative parameters of microstructural parameters

Tomographic and digital photographs of granulated and that of a healthy ‘Navel’ orange fruit are shown in Figure 3.6. Higher degree of granulation was observed on the tomographic images of ‘Navel’ orange, Fig 6a, while no granulation was observed in healthy ‘Navel’ orange, Fig 6b. The analysis further allowed for the derivation of other microstructural parameters including pore volume, area, specific area, porosity, skewness and kurtosis from each sample (Table 3.6). Following that, larger maximal pore volumes (0.85 cm^3) were detected in granulated fruit compared to healthy fruit. This yielded higher porosity in granulated fruit (2.02%) compared to the percentage porosity of healthy fruit (0.21%). Higher porosity as observed in granulated ‘Navel’ orange corresponded with the low moisture content of the fruit.

Herremans et al. (2014b) also observed a difference in microstructural parameters of health apple tissue and tissue affected by watercore. Their study reported higher pore volume, pore area, porosity and surface area to volume ratio in healthy apple tissue compared to watercore affected. Muziri et al. (2016) did not observe significant difference in the majority of morphometric parameters of X-ray tomographic images between mealy and non-mealy pear fruit, however, the total porosity percentage was significantly higher in mealy fruit compared to partly mealy and non-mealy fruit in the neck.

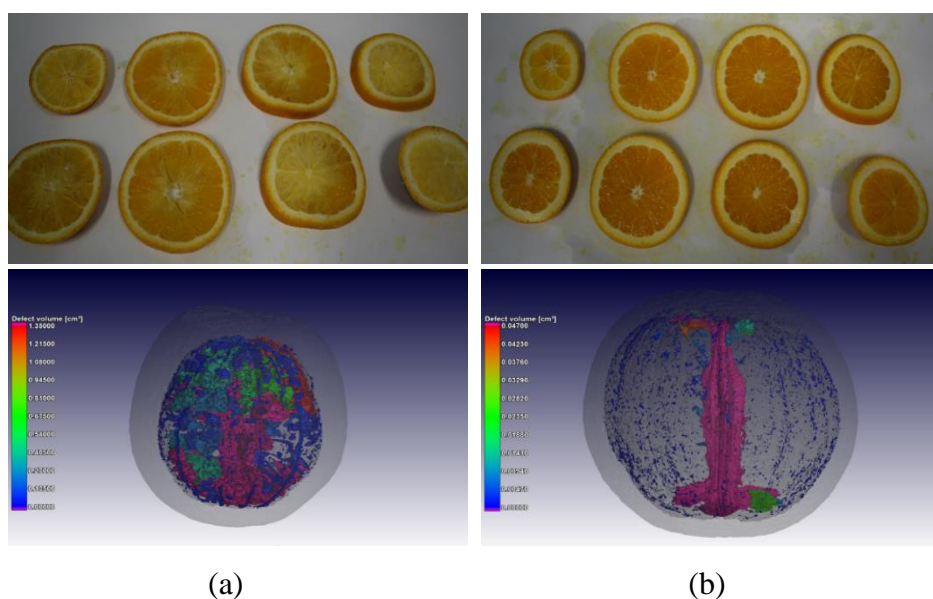


Figure 3.6 3D images of granulated and non-granulated ‘Navel’ orange

Table 3.6 Mean and standard deviation (SD) for 3D morphometric parameters of healthy and granulated ‘Navel’ orange samples

	Healthy fruit	Granulated fruit
N	9	21
Maximal cell volume (cm ³)	0.19 ±0.01 ^a	0.85±0.02 ^b
Cell area (cm ²)	0.01±0.00 ^a	0.03±0.01 ^b
Cell specific surface area (cm ⁻¹)	268.09±24.14 ^a	242.06±48.59 ^a
Porosity (%)	0.21±0.01 ^a	2.02±0.79 ^b
Skewness	29.86±2.12 ^a	20.27±0.36 ^a
Kurtosis	1386.71±51.86 ^a	595.91±43.55 ^b

3.3.3.3 Classification

The results of discriminant analysis presented in Table 7 indicated that the discriminant analysis could be used to distinguish between granulated and healthy tissue of ‘Navel’ orange based on tomographic images. Out of 30 ‘Navel’ fruit, 21 (were granulated and 9 non-granulated. A total of 26 samples (86.67%) were correctly classified. Using automated image threshold methods, Herremans et al. (2014b) correctly classified 68% and 89% watercore affected apples and healthy apples using maximum entropy and global threshold method respectively.

Table 3.7 Classification results for classification of ‘Navel’ orange fruit according to granulation and non-granulation based on 3D morphometric parameters.

	Class	Number	Correct	Granulated	Non-granulated
Class	Granulated	21	95.24%	20	1
	Non-granulated	9	66.67%	3	6

Classification success: 86.67%

3.4 Conclusions

Tomographic and radiographic images were able to reveal the presence of granulation in ‘Navel’ orange fruit. As an implication, this non-destructive imaging technique may be beneficial to postharvest handlers and processors of citrus fruit for early detection of granulation disorder. The classification of granulation based on tomographic images gave better results (86%) compared to radiographic images (70%). While tomographic imaging gave better results, both imaging techniques exhibited a greater degree of detecting granulation disorder in ‘Navel’ fruit. With reference to seeds detection, radiographic images could not reveal the presence of seeds in ‘Navel’ fruit; however, tomographic images were able to reveal ‘Navel’ seeds but had the limitation of not clearly separating the seeds from the endocarp due to a striking similarity between the two fruit part. Based on the present study, it may be important to consider improving the resolution of the tomographic images with other advanced models for seeds detection such as micro X-ray computed tomography.

References

- Arendse, E, Fawole, O. A., Magwaza, L. S., & Opara, U. L. (2016). Non-destructive characterization and volume estimation of pomegranate fruit external and internal morphological fractions using X-ray computed tomography. *Journal of Food Engineering*, 186, 42 – 49.
- Barcelon, E. G., Tojo, S., & Watanabe, J. (1999). X-ray computed tomography for internal quality evaluation of peaches. *Journal of Agricultural Engineering Research*, 73, 323 – 330.
- Barreiro, P., Zheng, C., Sun, D.-W, Hernandez-Sanchez, N., Perez-Sanchez, J. M., & Ruiz-Cabello, J. (2008). Non-destructive seed detection in mandarins: comparison of automatic threshold methods in FLASH and COMPIRA MRIs. *Postharvest Biology and Technology*, 47, 189 – 198.
- Cantre, D., Herremans, E., Verboven, P., Ampofo-Asiama, J., & Nicolai, B. (2014). Characterization of the 3-Dmicrostructure of mango (*Mangifera indica* L. cv. Carabao) during ripening using X-ray computed microtomography. *Innovative Food Science and Emerging Technologies*, 24, 28 – 39.
- Chao, C. C. T. (2005). Pollination study of mandarins and the effect of seediness and fruit size: Implications for seedless mandarin production. *American Society of Horticultural Science*, 40, 362 – 365.
- Chen, Q., Zhang, C., Zhao, J., & Ouyang, Q. (2013). Recent advances in emerging imaging techniques for non-destructive detection of food quality and safety. *Trends in Analytical Chemistry*, 52, 261–274.
- Chuang, C., Ouyang, C., Lin, T., Yang, M., Yang, E., Huang, T., Kuei, C., Luke, A., & Jiang, J. (2011). Automatic X-ray quarantine scanner and pest infestation detector for agricultural products, *Computers and Electronics in Agriculture*, 77, 41-59.
- du Plessis, A., Olawuyi, B. J., Boshof, W. P., & le Roux, S. G. (2014). Simple and fast porosity analysis of concrete using X-ray computed tomography. *Materials and Structures*, 49,553–562.

- Gueven, A., & Hicsasmaz, Z. (2013). Quantitative measurement of the pore structure. In: A. Gueven, & Z. Hicsasmaz (Eds), *Pore structure in food, simulation, measurement and applications* (pp.7-15). London, UK: Springer.
- Haff, R. P., & Pearson, T. C. (2007). An automatic algorithm for detection of infestations in X-ray images of agricultural products. *Sensing and Instrumentation for Food Quality and Safety*, 1, 143-150.
- Haff, R. P., & Toyofuku, N. (2008). X-ray detection of defects and contaminants in the food industry. *Sensing and Instrument for Food Quality and Safety*, 2, 262-273.
- Hernandez, N., Barreiro, P., Ruiz-Altisent, M, Ruiz-Cabello, J., & Fernandez-Valle, M. E. (2005). Detection of seeds in citrus using MRI under motion conditions and improvement with motion correction. *Concepts in Magnetic Resonance Part B: Magnetic Resonance Engineering*, 26 B, 81 – 92
- Hernandez-Sanchez, N., Barreiro, P., & Ruiz-Cabello, J. (2006). On-line identification of seeds in mandarins with magnetic resonance imaging. *Biosystems Engineering*, 95, 529 – 536.
- Herremans, E., Verboven, P., Bongaers, E., Estrade, P., Verlinden, B. E., Wevers, M., Hertog, M. L. A. T. M., Nicolai, B. M. (2013). Characterization of ‘Braeburn’ browning disorder by means of X-ray micro-CT, *Postharvest Biology and Technology*, 75, 114 – 124.
- Herremans, E., Verboven, P., Defraeye, T., Rogge, S., Ho, Q. T., Hertog, M. L. A. T. M., Verlinden, B. E., Bongaers, E., Wevers, M., and Nicolai, B. M. (2014a). X-ray CT for quantitative food microstructure engineering: The apple case, *Nuclear Instruments and Methods in Physics Research B*, 324, 88 – 94.
- Herremans, E., Melado-Herreros, A., Defraeya, T., Verlinden, B., Hertog, M., Verboven, P., Val., J., Fernandez-Valle, M. E., Bongaers, E., Estrade, P., Wevers, M., Barreiro, P., and Nicolai, B. M. (2014b). Comparison of X-ray CT and MRI of watercore disorder of different apple cultivars, *Postharvest Biology and Technology*, 87, 42 – 50.
- Jiang, J., Chang., H., Wu, K., Ouyang, C., Yang, M., Yang., E., Chen., T., & Lin, T. (2008). An adaptive image segmentation algorithm for X-ray quarantine inspection of selected fruits, *Computers and Electronics in Agriculture*, 60, 190 – 200.

- Jha, S. N., & Matsuoka, T. (2000). Non-destructive techniques for quality evaluation of intact fruits and vegetables. *Food Science Technology*, 6, 248-251.
- JinPing, X., LiGeng, C., Ming, X., HaiLin, L., & WeiQi, Y. (2009). Identification of AFLP fragments linked to seedlessness in Ponkan mandarin (*Citrus reticulata* Blanco) and conversion markers. *Scientia Horticulturae*, 121, 505 – 510.
- Kotwaliwale, N., Singh, K., Kalne, A., Jha, S. N., Seth, N., & Kar, A. (2014). X-ray imaging methods for international quality evaluation of agricultural produce, *Journal of Food Science and Technology*, 51, 1-15.
- Ladaniya, M. (2008). Fruit quality control, evaluation and analysis. In M. Ladaniya (Ed), *Citrus fruit: Biology, technology and evaluation* (pp.475-499). San Diego, CA: Elsevier Academic Press.
- Lammertyn, J., Dresselaers, T., Van Hecke, P., Jancsó, P., Wevers, M., & Nicolai, B. M. (2003). MRI and X-ray CT study of spatial distribution of core breakdown in ‘Conference’ pears, *Magnetic Resonance Imaging*, 21, 805 - 815.
- Lin, T., Jiang, J., Ouyang, C., & Chang, H. (2005). Integration of an automatic X-ray scanning system for fruit quarantine. In *The eighth international conference on automation technology conference*, Taichung, Taiwan, 1-6.
- Magwaza, L. S., & Opara, U. L. (2014). Investigating non-destructive quantification and characterization of pomegranate fruit internal structure using X-ray computed tomography. *Postharvest Biology and Technology*, 95, 1 – 6.
- Nicolai, B. M., Bulens, I., Josse De Baerdemaeker, DeKetelaere, B., Hertog, M. L.A.T. M., Verboven, P., & Lammertyn, J. (2009). Non-destructive evaluation: Detection of external and internal attributes frequently associated with quality and damage. In: *Postharvest Handling: A Systems Approach*, Florkowski, W. J., Shewfelt, R. L., Brueckner, B., and Prussia, S. E., Eds. London, UK: Elsevier, 421-441
- Nicolai, B., Defraeye, T., De Ketelaere, B., Herremans, E., Hertog, M. L. A. T. M., Saeys, W., Torricelli, A., Vandendriessche, T., & Verboven, P. (2014). Non-destructive measurement of fruit and vegetable quality, *Annual Review Food Science Technology*, 5, 285 – 312.

- Nielsen, M. S., Christensen, L. B., & Feidenhans'l, R. (2014). Frozen and defrosted fruit revealed with X-ray dark-field radiography. *Food Control*, 39, 222 – 226.
- Muziri, T., Theron, K. I., Cantre, D., Wang, Z., Verboven, P., Nicolai, B.M., & Crouch, E.M. (2016). Microstructure analysis and detection of mealiness in 'Forelle' pear (*Pyrus communis* L.) by means of X-ray computed tomography, *Postharvest Biology and Technology*, 120, 145–156.
- Peiris, K. H. S., Dull, G. G., & R. G. Leffler. (1998). Nondestructive detection of section drying, an internal disorder in tangerine. *HortScience*, 33, 310 – 312.
- Raza, H., Khan, M. M., & Khan, K. K. (2003). Seedlessness in citrus. *International Journal of Agriculture and Biology*, 5, 388 – 391.
- Ritenour, M. A. (2004). Granulation in Florida citrus. *Proceedings of the Florida State Horticultural Society*, 117, 358-361.
- Sharma, R. R., & Saxena, S. K. (2004). Rootstocks influence granulation in Kinnow mandarin (*Citrusnobilis*×*C. deliciosa*). *Scientia Horticulturae*, 101, 235–242.
- Sharma, R. R., Singh, R., & Saxena, S. K. (2006). Characteristics of citrus fruits in relation to granulation. *Scientia Horticulturae*, 111, 91-96.
- Sikuka, W. (2015). South Africa citrus annual report, Global Agricultural Information Network [online], June 15 2015. Available: http://gain.fas.usda.gov/Recent%20GAIN%20Publications/Citrus%20Semi-annual_Pretoria_South%20Africa%20-%20Republic%20of_6-15-2015.pdf
- van Dael, M., Lebotsa., S., Herremans, E., Verboven, P., Sijbers, J., Opara., U. L., Cronje, P. J., & Nicolai, B. M. (2016). A segmentation and classification algorithm for online detection of internal disorders in citrus using X-ray radiographs, *Postharvest Biology and Technology*, 112, 205-214.
- Vicente, A. R., Manganaris, G. A., Sozzi., G. O., & Crisosto, C. H. (2009). Nutritional Quality of Fruits and Vegetables, In W. J. Florkowski, R. L. Shewfelt, B. Brueckner, and S. E. Prussia (Eds), *Postharvest Handling: A Systems Approach* (pp.57-106). Lodon, UK: Elsevier.

Zhang, J., Wang, M., Cheng, F., Dai, C., Sun, Y., Lu, J., Huang, Y., Lia, M., He, Y., Wang, F., & Fana, B. (2016). Identification of microRNAs correlated with citrus granulation based on bioinformatics and molecular biology analysis, *Postharvest Biology and Technology*, 118, 59 - 67.

Zou, Z., Xi, W., Hu, Y., Nie, C., & Zhou, Z. (2016). Antioxidant activity in citrus fruits. *Food Chemistry*, 196, 885-896.

4. Classification of ‘Satsuma’ mandarin fruit based on physicochemical quality attributes using near infrared spectroscopy

Abstract

The study aimed to investigate influence of the position of fruit during scanning on near infrared (NIR) spectroscopy model prediction accuracy and to classify ‘Satsuma’ mandarin fruit based on physicochemical attributes predicted. Reflectance NIR spectral data was acquired from six different positions within a fruit; four from equatorial spots of the fruit and two from the stem-end and the styler-end of the fruit. Reference measurements included fruit mass, firmness, vitamin C, total soluble solids (TSS), titratable acidity (TA), pH, citrus colour index (CCI), and hue angle (h^*). Partial least square (PLS) regression analysis was used to develop prediction models. Orthogonal PLS discriminant analysis (OPLS-DA) was used to test the possibility of PLS models to distinguish between two groups based on physicochemical quality attributes. Models were evaluated based on coefficient of determination (R^2), bias and root mean square error of cross validation (RMSECV), root mean square error of prediction (RMSEP), and the residual predictive deviation (RPD). Prediction models developed from six scan positions were compared to those developed from only the four equatorial positions and those developed from one scan position per fruit. Position of fruit during scanning had an influence on model prediction accuracy with four scan positions (equatorial positions) giving better results. Calibration and validation for the 4 scan positions yielded for mass ($R^2 = 94.42$, RMSEP = 7.86 g and RDP = 3.46), TSS ($R^2 = 73.81$, RMSEP = 1.37 and RPD = 1.95), TA ($R^2 = 70.72$, RMSEP = 0.136 and RPD = 1.64), and for h^* ($R^2 = 79.17$, RMSEP = 4.78 and RPD = 1.96). For the classification of high and low values of quality attributes, the results showed classification accuracies of above 87% for both calibration and validation.

Keywords:

Classification, scan position, PLS, OPLS-DA

4.1 Introduction

Quality monitoring of fruit produce is of vital importance at every stage from harvest to market (Lurie, 2009; Kotwaliwale et al., 2014; Wang & Xie, 2014). Quality comprises properties such as sensory attributes (which include appearance, texture, taste and aroma), nutritive values, chemical composition, mechanical and functional properties as well as absence of defects (Abbott et al., 1999). Citrus fruit quality, in particular, includes external quality requirements such as shape, colour, lack of blemishes and disorders and internal quality factors, which include the percentage of juice, sugar and acid content as per product quality standards provided by Department of Agriculture, Forestry and Fisheries (DAFF, 2012; DAFF, 2016). Instrumental measurements of these properties are preferred over sensory evaluations due to variations among individuals in sensory evaluations (Abbott et al., 1999).

Various techniques for quality evaluation in the fruit industry have been reported. There are destructive and non-destructive methods, the latter being more advantageous than the former (Lurie, 2009; Nicolai et al., 2007; Nicolai et al., 2014). The trend in the agricultural industry is moving away from destructive measurements to non-destructive measurement of quality (Lurie, 2009; Kotwaliwale et al., 2014). Near infrared (NIR) spectroscopy, in particular, has been successfully applied to study the internal quality of fruit such as ‘Satsuma’ mandarin (McGlone et al., 2003; Gomez et al., 2006), other mandarins (Guthrie et al., 2005a, b; Liu et al., 2010; Sanchez et al., 2013; Magwaza et al., 2014a, b, c), other citrus varieties such as ‘Valencia’ orange (Cayuela 2008; Cayuela & Weiland, 2010; Magwaza et al., 2013), and ‘Navel’ orange (Wang et al., 2014).

Among studies available in the literature reporting the use of NIR spectroscopy for quality analysis, there are limited reports on ‘Satsuma’ mandarin. McGlone et al. (2003) compared different measurement modes (reflectance, interactance and transmission) to predict total soluble solids (TSS) of ‘Satsuma’ mandarin. Gomez et al. (2006) successfully evaluated the use of visible (vis) to near infrared (vis/NIRS) spectroscopy to measure TSS, pH and compression force of ‘Satsuma’ mandarin. Fraser et al. (2003) studied the light distribution inside mandarin fruit during internal quality measurement by NIR spectroscopy.

Various factors may affect the performance of NIR to detect fruit quality parameters. One such factor may be the positioning of the fruit during NIR scanning due to variation in quality attributes within the fruit. Walsh (2005) highlighted that the accuracy of NIR spectroscopy is

limited by non-homogeneity of the attribute of interest in the fruit. Guthrie et al. (2005a) reported a variation of TSS in 'Imperial' mandarin fruit, increasing from proximal end (stem-end) to distal end (styler-end), and decreasing from skin (peel) to core. Both authors compared models performances based on the point at which fruit is scanned during spectral acquisition and found that the stem-end gave poor prediction models when compared to those obtained from the equatorial and styler-ends. Despite these results, the effect of the point at which fruit is scanned on NIR calibration model performance in 'Satsuma' mandarin has not been investigated. These aspects can be of particular relevance in the application of NIR spectroscopy for on-line sorting. Therefore, one of the aims of the study was to investigate the effect of positioning of fruit during scanning, for qualitative and quantitative evaluation of the physicochemical quality attributes of 'Satsuma' mandarin. Magwaza et al. (2012a) and Walsh (2005) highlighted that the limited penetration depth of NIR decreases the accuracy of NIRS to measure internal quality attributes of fruit with thick peel such as citrus. In addition to position of fruit during scanning, the effect of 'Satsuma' mandarin peel for qualitative evaluation of the quality attributes was investigated.

Fruit may need to be separated into classes depending on product quality standards or target market specifications. Also, presentation of fruit to consumers in homogeneous categories has significant effect on consumer decision (Blasco et al., 2003). Blasco et al. (2003) reported that several manufacturers worldwide produce sorting machines capable of pre-grading fruits by size, colour and weight. Taste is regarded as an important internal quality parameter of fruits and is influenced by sugar and acid levels (Abu-Khalaf & Bennedsen, 2004; Jamshidi et al., 2012; Magwaza & Opara, 2015). Sugar level also serves as a measure for fruit maturity (Zude et al., 2008). Therefore in addition to detection of quality parameters, the study also aimed to classify 'Satsuma' mandarin fruit based on quality parameters according to mass, sugar content (total soluble solids), acidity (total acidity) and colour (hue angle).

4.2 Materials and methods

4.2.1 Site and sample collection

A total of 160 ‘Satsuma’ mandarin (*Citrus unshui*) fruit was harvested from an orchard at the experimental farm of Stellenbosch University, Western Cape, South Africa (33°53'4.66" S, 18°37'36.84" E). During sampling, eight trees were randomly selected. Fruits were sampled from the sun exposed canopy position on some trees, and from the shaded canopy position on other trees. Of each of the twenty fruit per canopy position, ten were green and the other ten were yellow in colour at the time of harvest. In addition, the fruits were selected in such a way that each lot per canopy position included five small mandarins and five bigger fruits. The fruits were labelled and combined, but each fruit was considered as an experimental unit. The fruits were harvested in April 2011 and transported overnight to the laboratory and stored at room temperature (20°C) before spectral measurements with the NIR instrument were taken the following morning.

4.2.2 NIR spectral acquisition

The Multiple Purpose AnalyzerTM (MPA) Fourier transform NIR spectrometer (Bruker Optics, Ettlingen, Germany), fitted with OPUS software for Windows (OPUS version 7.2, Bruker Optics, Ettlingen, Germany), was used to generate reflectance (R) spectra of ‘Satsuma’ mandarin fruit in the wavelength range 800.44 nm – 2779.32 nm. The spectral resolution was 8 nm. Measurements were done on a rotating integrating sphere in reflectance mode. Each fruit was placed directly above the rotation integrating sphere of the spectrometer and scanned individually (Figure 4.1). Reflectance measurements were transformed to absorbance ($\log(1/R)$) in OPUS software, in order to linearise the correlation between the NIR values and the actual values of the reference data. Graphic displays of the spectra were shown as absorbance.

Reflectance spectra were acquired from six positions on each fruit by manually turning the fruit on the rotating integrating sphere. Four spectra were collected from evenly spaced equatorial spots on the fruit and one each from the stem-end and the stylar-end of the fruit. First, a fruit was placed above the point of measure, with the stem-end and scanned. The fruit was then turned manually and placed above the point of measurement with the stylar-end and scanned. Following this, the fruit was turned and positioned above the point of measurement with stylar-end to stem end axis horizontal to measure the four equatorial points of the fruit.

A total of 32 scans per point of measurement were conducted and averaged. The fruits were stored in a cold room with a delivery air temperature of 4°C overnight before further measurements the following morning. Fruits were then allowed to equilibrate at room temperature, after which physicochemical measurements were taken.



Figure 4.1 NIR spectral acquisition setup showing the position of fruit during scanning, with fruit placed directly above the rotation integrating sphere to scan the stylar-end.

4.2.3 Physicochemical measurements

The fruit was weighed using a calibrated weighing balance (Mettler Toledo, Columbus, Ohio, $\pm 0.01\text{g}$). Rind colour components were measured in three values using the International Commission on Illumination (CIE) X, Y and Z colour space with a Minolta CR-400 colorimeter (Chroma Meter CR-400, Konica Minolta Sensing Inc., Japan) after calibration using a standard white tile (CR-A43; $Y = 93.1$, $x = 0.3138$; $y = 0.3203$) according to the method by Magwaza et al. (2012b). The colour measurements were taken at a point along the equatorial axis of each fruit. The values were transformed to CIE L^* , a^* , b^* coordinates, which according to Abbott et al. (1999) provide uniform colour differences in relation to human perception. From a^* and b^* colour parameters, hue angle (h^*) was calculated using Eq. 1 (Pathare et al., 2013).

$$h^* = \tan^{-1}(b^*/a^*) \quad (1)$$

Titrateable acidity (TA) was measured by titrating 2 mL of fresh juice against 0.1M sodium hydroxide (NaOH) to an end point of pH 8.2 using a titrosampler (Metrohm 862 compact, Herisau, Switzerland) as described by Magwaza et al. (2013). Total soluble solid (TSS) was measured using a digital refractometer (Atago, Tokyo, Japan) and the results were expressed as Brix. All the measurements were done in duplicates (two measurements per sample) and averaged.

4.2.4 Data Analysis

4.2.4.1 Partial least squares calibration procedure

Partial least squares (PLS) regression analysis was carried out to construct calibration models for predicting the quality parameters, mass, hue angle (h^*), total soluble solids (TSS), and titrateable acidity (TA). Three sets of models were developed. The first set of calibration models were developed from six spectra of each fruit, followed with second set with only four of the six spectra which consisted of only spectra of equatorial positions of each fruit. The third set of prediction models was performed with one spectrum of each fruit and data set were designed to have an equal distribution of stylar-end, stem-end, and equatorial positions. During model development, the spectra were averaged, e.g for six scan positions the six spectra per fruit were averaged.

Acquired spectra were processed using OPUS software. Calibrations models were developed using PLS regression and segmented cross validation (20 randomly selected samples per segment for each iterative calculation). Models were optimised on the basis of the root mean square error of cross-validation (RMSECV), spectral pre-processing that included various combinations of spectral transformations (e.g. raw, first and second derivatives, standard normal variate (SVN), min-max normalization (MMN), multiplicative scattering correction (MSC), straight line subtraction (SLS) and constant offset elimination (COE)), and a selection of wavelength ranges. The main aim of spectral pre-processing is to remove unwanted signals to enhance the efficiency of prediction models (Rinnan et al., 2009). The combination of optimisation methods which gave the lowest RMSECV per parameter was selected.

Criteria for evaluating the performance of models were based on coefficient of determination (R^2), bias and RMSECV. These statistics are used extensively in NIR spectroscopy and have been described in Eriksson et al. (2006). In evaluating the prediction models, the guidelines

provided by Saeys et al. (2005) were used: R^2 value between 0.66 and 0.81 indicates accurate quantitative predictions, whereas, R^2 value between 0.82 and 0.90 suggests good prediction.

4.2.4.2 Validation procedure

The performance of the calibration models was assessed by independent test set validation for which 30% of the samples were used. Evaluation was based on root square error of prediction (RMSEP), R^2 and the residual predictive deviation (RPD). RPD is defined as the ratio of standard deviation of the reference data for the validation dataset to the RMSEP (Williams & Sobering, 1996). Saeys et al. (2005) and Nicolai et al. (2007) reported that RDP values below 1.5 indicate that the calibration is not usable; between 1.5 and 2.0 indicates a possibility to distinguish between high and low values, while a value between 2.0 and 2.5 makes good predictions possible. RPD values between 2.5 and 3.0, and above, indicate good and excellent predictions, respectively.

4.2.4.3 Orthogonal partial least square-discriminant analysis

Discriminant analysis is a supervised classification method primarily used to build classification rules for pre-specified subgroups, or classes, in a set of samples (Eriksson et al., 2006). The rules are then used to allocate future unknown samples to the most probable subgroup. In this study, a two-class discriminant analysis was used to distinguish between a priori “low” and “high” classes of ‘Satsuma’ mandarin fruit, for each of the quality parameters: mass, hue angle (h^*), total soluble solids (TSS), and titratable acidity (TA). Samples belonging to “low” and “high” classes were identified on the basis of the predicted quantitative values obtained with the PLS models developed in this study. The export standards and requirements provided by DAFF (2016) were used as a guideline for the demarcation of the range of values to be used in defining each class.

Two-class (low vs. high) discrimination was done using the OPLS-DA function in SIMCA version 14 (Umetrics, Umeå, Sweden). Averaged mandarin fruit NIR spectra as described before, were mean-centred. The wavelengths at which the fruit absorbance was measured were used as input x -variables and a dummy variable denoting low or high class membership, respectively, as input y -variables. The actual absorbance values of each fruit were considered as the observations (samples). Separate models were built for each of the quality parameters. OPLS-DA has been described (Wiklund et al., 2008) and has an advantage over PLS-DA in that the model is rotated so that the variation correlating to class separation is projected on the

first predictive component [t1]. Variation that is uncorrelated with class separation is projected on one or more orthogonal components [to]. The outputs of the discriminant analysis in this study were visualised in scores scatter plots and S-line plots. In the 2-D scores scatter plots, the between-class variation was projected on the predictive component (horizontal direction), and the within-class variation on the orthogonal component(s) (vertical direction). The separation of predictive and orthogonal components aided the interpretation of the discrimination between low and high classes. Furthermore, since it was of interest to interpret the influence of the x -variables on the between-class (low vs. high) and within-class variation, the loadings plots were visualised as S-line plots. These plots combine covariance and correlation loadings obtained from the predictive component, [t1], of the OPLS-DA models (Wiklund et al., 2008) and thereby identify the wavelengths that are important for the separation between low and high classes.

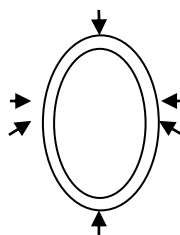
The OPLS-DA models were validated with independent test set validation using 50% of the samples in test sets. For each data set, the selection of data ensured that both training and tests sets contained an equal number of low and high samples. Classification accuracies were extracted to show the proportion of correctly classified observations per quality parameter.

4.2.4.4 Analysis of variance

The distribution statistics (range, mean and standard deviation) of the physicochemical reference values were calculated for the different sets of data used for OPLS-DA. One way Analysis of Variance (ANOVA) was performed to identify statistically significant differences ($p < 0.05$) between the means of reference values. ANOVA was done using Microsoft Excel 2010 (Microsoft, Redmond, USA).

Sample collection:**Sample scanning positions:**

6 scan positions on intact 'Satsuma' mandarin

**Reference data:**

Mass

TSS

TA

h^*

Data analysis

PLS models: 1) 6 scan positions

2) 4 scan positions

3) 1 scan position

OPLS-DA

ANOVA

Figure 4.2 Summary of methodology comprising sample collection, scanning of samples, reference data collected, partial least squares (PLS) prediction models, orthogonal partial least squares–discriminant analysis (OPLS-DA) and analysis of variance (ANOVA). TSS is the total soluble solids, TA is titratable acidity, h^* is hue angle, OPLS-DA, Orthogonal partial least squares-discriminant analysis, PLS, Partial least squares, ANOVA, analysis of variance.

4.3 Results and discussion

4.3.1 Spectral analysis

The original fruit spectra were collected in reflectance mode, and the absorbance intensities in Figure 4.3 are in accordance with literature reports (Gomez et al., 2006; Magwaza et al., 2011). The typical spectrum of one intact ‘Satsuma’ mandarin fruit featured five peaks in the regions of 980, 1200, 1460, 1790 and 1930 nm (Fig.3). The peak at 980 nm could be ascribed to absorption by water and carbohydrates, as described (Gomez et al., 2006; Xudong et al., 2009). This peak was expected, since about 80 – 90% of fruit mass consists of water (McGlone et al., 2003; Gomez et al., 2006). In the region of 1200 nm, first harmonic of OH combination band occurs (McGlone et al., 2003).

According to Miller & Miller (2010), strong water absorption also occurs in the region 1400 –1600 nm and therefore the prominent peak occurring at 1460 nm can be attributed to water absorbance. The peak at 1790 nm overlaps with carbohydrate absorbance (Louw & Theron, 2010). The spectral pattern and peak characteristics of the spectrum were similar to those previously obtained for ‘Satsuma’ mandarin (Gomez et al., 2006), and for intact oranges (Cayuela & Weiland, 2010; Magwaza et al., 2011).

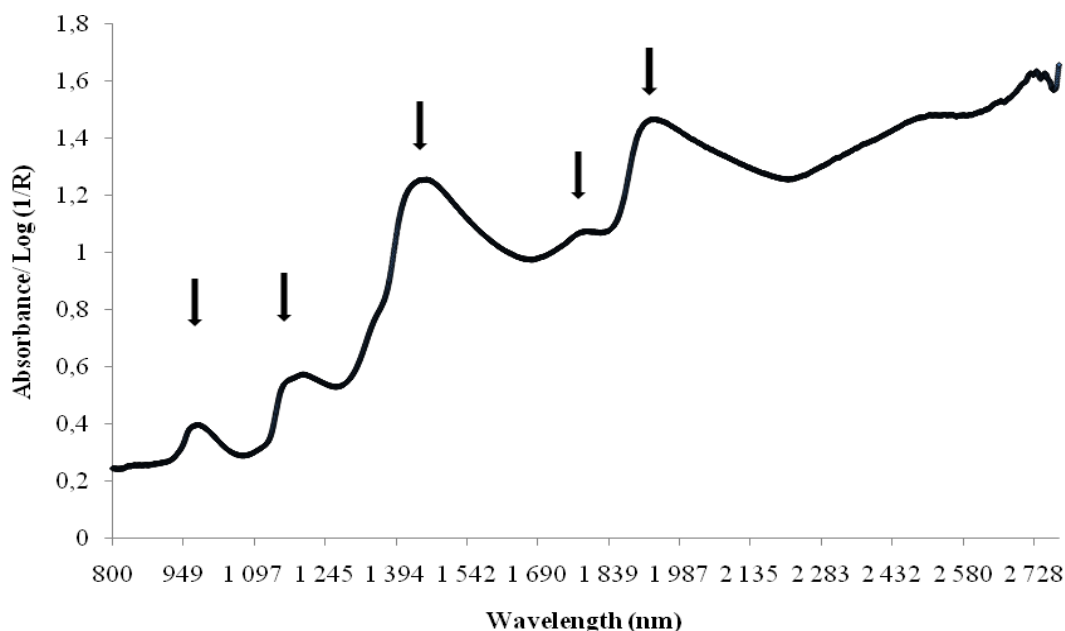


Figure 4.3 Typical raw Fourier transform NIR spectrum of one intact ‘Satsuma’ mandarin fruit in the wavelength range 800.44 nm – 2779.32 nm.

4.3.2 NIR based PLS calibration and validation models

Table 4.1 displays the statistics for PLS calibration models that were developed with respectively, six spectra (four taken from equatorial spots of the fruit and one each from the stem-end and the styler-end of the fruit), four spectra (only the equatorial spots on the fruit) and one spectrum of each fruit. The six and four spectra data were averaged during development of models. The regression statistics obtained with each of these sets of data are discussed separately below.

Six spectra per fruit

The calibration statistics for mass yielded R^2 of 0.85 and RMSECV of 10.6 g, with prediction results yielding a RMSEP value of 11.9 g and RPD of 2.35 (Table 4.1). The results showed an improvement to those obtained by Sanchez et al. (2013) for ‘Clemevilla’ mandarin, who obtained an R^2 of 0.53, SECV of 24.31 g and SEP of 26.12 g.

The calibration statistics for TSS were $R^2 = 0.69$ and RMSECV = 1.37 °Brix. The prediction results of the test set validation yielded RMSEP of 1.4 °Brix and RPD of 1.67. Better results were obtained for ‘Satsuma’ mandarin by McGlone et al. (2003) with validation statistics of $R^2 = 0.93$, RMSEP = 0.32 °Brix and by Wang et al. (2014) for orange with an R^2 of 0.89, RMSECV = 0.43 and RMSEP = 0.46 °Brix.

Calibration statistics for h^* were $R^2 = 0.71$ and RMSECV = 4.28. Prediction results of the test set validation yielded RMSEP of 4.3 and RPD = 1.76. The results yielded a lower R^2 but an improved RMSECV compared to Sanchez et al. (2013) who obtained R^2 of 0.79, SECV of 5.71 and SEP of 6.55 for mandarin.

Results for TA were $R^2 = 0.51$ and RMSECV = 0.17% with validation statistics of $r^2 = 0.34$ and RMSEP = 0.18% and RPD = 1.26. The results are comparable to those obtained by McGlone (2003) for TA in ‘Satsuma’ mandarin with R^2 of 0.6 and RMSEP of 0.15%.

Models with RPD values above 1.5 were reported to have a possibility to distinguish between high and low values (Saeys et al., 2005; Nicolai et al., 2007). Ranking the results according to RPD values, Table 1 shows that for six scan positions, mass ranked first with an RPD value of 2.35. This was followed by h^* which yielded RPD = 1.76. TSS gave RPD of 1.67, while TA yielded RPD of 1.26. The RPD values were all greater than 1.5 except for TA.

Four spectra: Due to a large variation in quality parameter distribution in the stylar-end and stem-end as reported by Guthrie et al. (2005a), the effects of exclusion of these scan positions on the prediction models were investigated. Models developed from the four equatorial positions were compared to those developed from the six scan positions. Better results were obtained with four scan positions for all the quality parameters (Table 4.1). For example, mass yielded R^2 of 0.94, RMSECV of 6.69 g, with prediction results of RMSEP = 7.86 g and RPD = 3.46 compared to calibration results of R^2 of 0.85 and RMSECV of 10.6 g, with prediction results of RMSEP of 11.9 g and RPD of 2.35. All the parameters yielded RPD value greater than 1.5. Mass in this case also ranked first, followed by h^* , TSS, then TA.

The improvement in results when only the four equatorial positions show that the two end parts, the stem-end and stylar-end, do not contain much information about the internal quality and that by averaging 6 spots, the quality of the information captured in the spectra is compromised. Guthrie et al. (2005) reported a lower coefficient of variation in TSS at equatorial circumference compared to stylar-end and stem-end.

One spectrum: Collecting a single spectrum per fruit may save time during quality monitoring in the packhouse and therefore models from one scan position were developed. Bearing in mind that controlling the manner in which fruit moves along a conveyor belt may not be possible, data set were designed to have equal distribution of stylar-end, stem-end, and equatorial positions. Models were developed from a data set where only one spectrum per fruit was included. Comparing these results to those developed from six spectra, the models did not perform better for all the quality parameters with mass yielding $R^2 = 0.71$, RMSECV = 15.00 g and prediction results of RMSEP = 16.90 g and RPD = 1.70 compared to R^2 of 0.85 and RMSECV of 10.6 g, with prediction results yielding RMSEP of 11.9 g and RPD of 2.35 (Table 4.1).

In contrary to models developed from six scan positions, using only one scan per fruit did not improve the models and only mass yielded RPD value of greater than 1.5 while the other quality parameters RPD were less than 1.5. The RPD value of mass (1.7) shows that for mass, classification can still be obtained by scanning the fruit once. These results therefore indicate that single spectrum per fruit may not be a good representative of the entire fruit hence there was no improvement when only one spectrum per fruit was used.

Table 4.1 PLS model statistics for 6, 4 and 1 scanning positions) as determined from NIR spectra and reference physicochemical measurements

		Calibration			Validation			Waveband (nm)	
		R ²	RMSECV	Bias	r ²	RMSEP	RPD		
6 scan positions	Mass (g)	0.85	10.60	0.17	0.81	11.90	2.35	MSC	6102-5446.3
	TSS (⁰ Brix)	0.69	1.37	-0.12	0.64	1.40	1.67	SNV	9403.7-6098.1; 5025.8-4597.7
	h*	0.71	4.28	0.16	0.66	4.30	1.76	1 st derivative+MSC	9403.7-7498.3; 6102-5774.1; 4601.6-4424.1
	TA (%)	0.51	0.17	-0.003	0.34	0.18	1.26	1 st derivative+MSC	9403.7-8451
4 scan positions	Mass (g)	0.94	6.69	-0.20	0.91	7.86	3.46	COE	9403.7-4597.7
	TSS (⁰ Brix)	0.74	1.24	-0.13	0.74	1.37	1.95	MSC	9403.7-6098.1; 4601.6-4246.7
	h*	0.79	4.70	-0.45	0.73	4.78	1.96	COE	7502.1-5446.3
1 scan position	TA (%)	0.71	0.13	-0.002	0.63	0.14	1.64	MMN	9403.7-7498.3; 4601.6-4246.7
	Mass (g)	0.71	15.00	-0.06	0.65	16.90	1.70	COE	9403.6-7498.2; 6101.9-4597.7
	TSS (⁰ Brix)	0.62	1.62	-0.07	0.53	1.72	1.49	MSC	9403.6-7498.2; 6101.9-4597.7
	h*	0.61	6.54	0.12	0.47	7.39	1.42	1 st derivative+SNV	1 st derivative+SNV
	TA (%)	0.47	0.224	-0.009	0.40	0.26	1.31	MMN	6101.9-4597.7

R²: Coefficient of determination, RMSECV: root mean square error of cross validation (same units as quality parameter), RMSEP: root mean square error of prediction (same units as quality parameter), RPD: ratio of prediction to deviation, MSC: Multiplicative scattering correction, SLS: Straight line correlation, MMN: Min max normalization, COE: Constant offset elimination, SNV: Standard normal variate, RPD: residual predictive deviation, R²: coefficient of determination, TSS: total soluble solids, TA: titratable acidity, h*: hue angle.

4.3.3 Fruit classification with orthogonal partial least square-discriminant analysis

4.3.3.1 Classification data distribution

Predicted values of quality parameters were divided into two ranges, the high values and the low values, for classification. Based on export standards and requirements provided by DAFF (2016), the minimum requirement for TSS is 8.5 °Brix for ‘Satsuma’ mandarin. To develop the classification criteria for TSS, values could be separated at 8.5 °Brix, but due to prediction error of RMSEP = 1.4 °Brix (Table 4.1), values of 7 °Brix and less were classified as low and values of 10 °Brix and above were classified as high. Standard for colour is based on colour charts made available to pack houses (DAFF, 2016). The criteria for h^* was therefore based on hue angle colour chart, with 60° representing yellow, 90° representing lime and 120° representing green. Again taking into consideration prediction error (RMSEP = 4.3), values below 80° were classified as low and values above 90° as high. However, for mass, there are no specific requirements outlined, and classification was explored. OPLS-DA was used to analyse predicted values for classification based on the quality parameters (TSS, mass and h^*).

The distribution statistics for the reference data for six scan positions are summarised in Table 4.2. Mass, TSS, and h^* means were significantly different between each of the classes ($p < 0.05$). The significant difference demonstrated that the data indeed belong to different groups.

Table 4.2 Range, mean and standard deviation (SD) for mass, TSS and h* for two sets of classes of each of the quality parameters. Values for comparing the two classes for each quality attribute are reported with different letters next to them in the same column.

Quality parameters	Class	Range	Mean \pm SD
Mass (g)	1	≥ 100	100.60-161.27 116.39 \pm 2.09 ^a
	2	≤ 50	23.74-49.88 42.50 \pm 1.12 ^b
TSS (Brix)	1	≥ 10	10.00-14.90 11.54 \pm 0.15 ^a
	2	≤ 7	3.10-7.00 5.18 \pm 0.22 ^b
h*	1	≤ 70	64.98-79.61 73.65 \pm 0.58 ^a
	2	≥ 90	90.30-111.29 99.23 \pm 0.84 ^b

TSS: total soluble solids, h*: hue angle.

4.3.3.2 Classification

The results of 2-class discrimination using OPLS-DA indicated that the models can separate between low values and high values for mass, TSS and h* when using all the six spectra from each fruit. Figure 4.4a, Figure 4.4b and Figure 4.4c showed clear separation between low values (L, represented with green colour) and high values (H, represented with blue colour) for mass, h* and TSS.

Classification results showed the proportion of correctly classified observations in the calibration as well as validation sets. In terms of TSS calibration, 96.03% of low values were correctly classified and 98.72% of high values were correctly classified and 96.3% low class and 93.64 high class correct classifications for validation (Table 4.3). 100% of low values and 100% for h* calibration were correctly classified, with validation yielding 98.82% and 100% correct classification for low and high values respectively. The results for mass yielded 90% correct classification for low values of mass and 100% correct classification for high values. During validation, 87.86% low values were correctly classified while 100% high values were correctly classified. The results showed that NIR spectroscopy can be used as a tool to classify fruit according to TSS content and surface colour.

The corresponding S-line plots in Figure 4.4 showed the spectral regions which contributed to the class separation. The high numerical values with a red colour are spectral regions of high correlation with class discriminating power. The S-line plot identified the NIR wavebands responsible for discrimination, with the regions 6985.19 – 7112.48 cm^{-1} for TSS, 5299.65-5326.65 and 9905.01-10121.00 for h^* while region for mass was 8821.17-9816.3 cm^{-1} .

Table 4.3 ‘Satsuma’ mandarin OPLS-DA classification table for test set validation according to low (L) and high values (class H) of TSS and h^*

	Quality parameter	Class	Number	Correct	L	H
Class	TSS	L	135	96.3%	130	5
		H	236	93.64%	15	221
	h^*	H	85	98.82%	84	1
		L	77	100%	0	77
	Mass	H	173	87.86	152	21
		L	185	100	0	185

L: low values, H: high values, TSS: total soluble solids, h^* : hue angle.

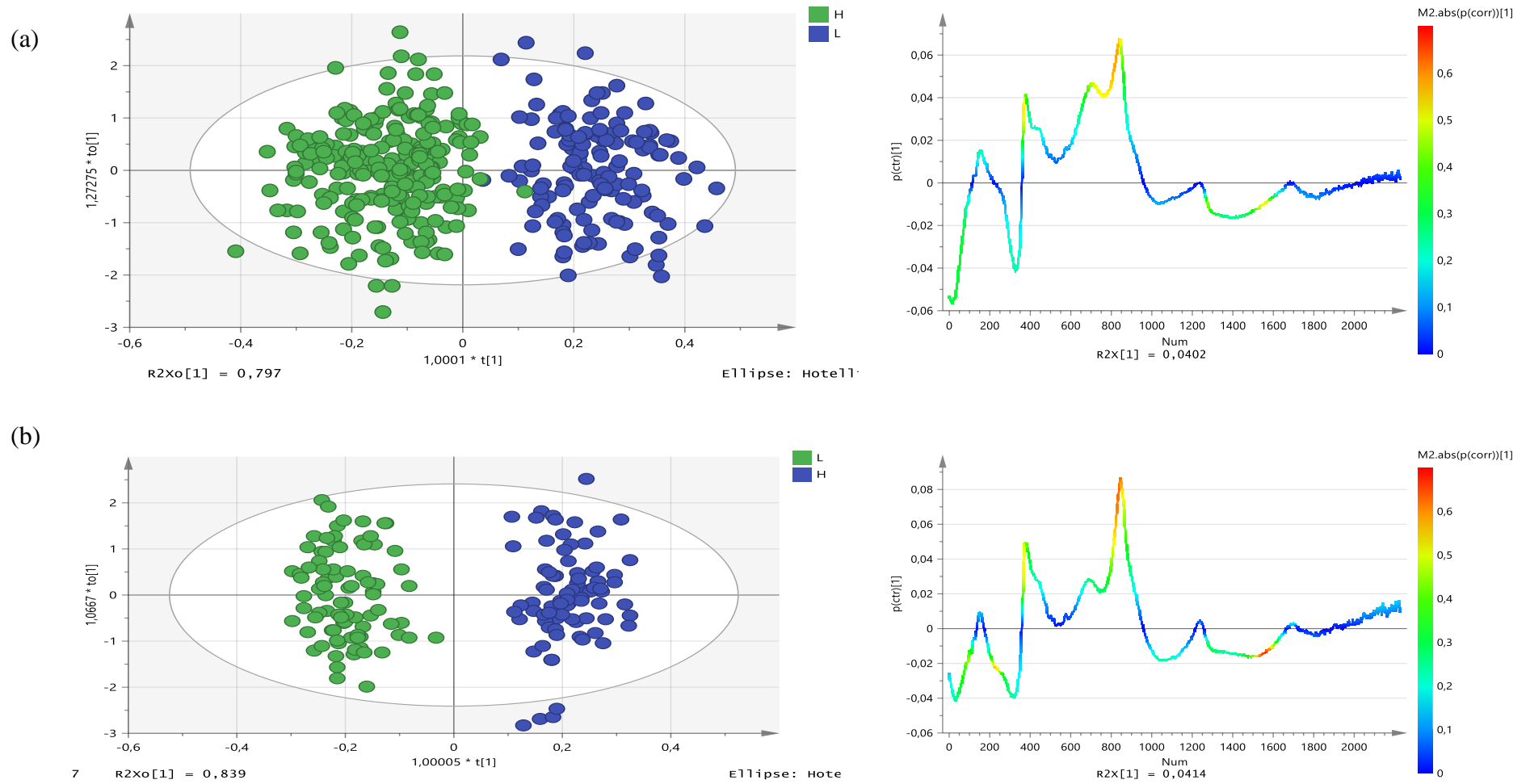


Figure 4.4 OPLS-DA plots, for TSS (a), h^* (b), and Mass (c), with scatter score plots on the left and corresponding S-line plots on the right.

TSS classes L: 4 – 8 °Brix, H: 9.1 – 15 °Brix, h^* classes L: 60 – 75 °, H: 75.1 – 120 °, Mass classes L:23-60, H: 90-162

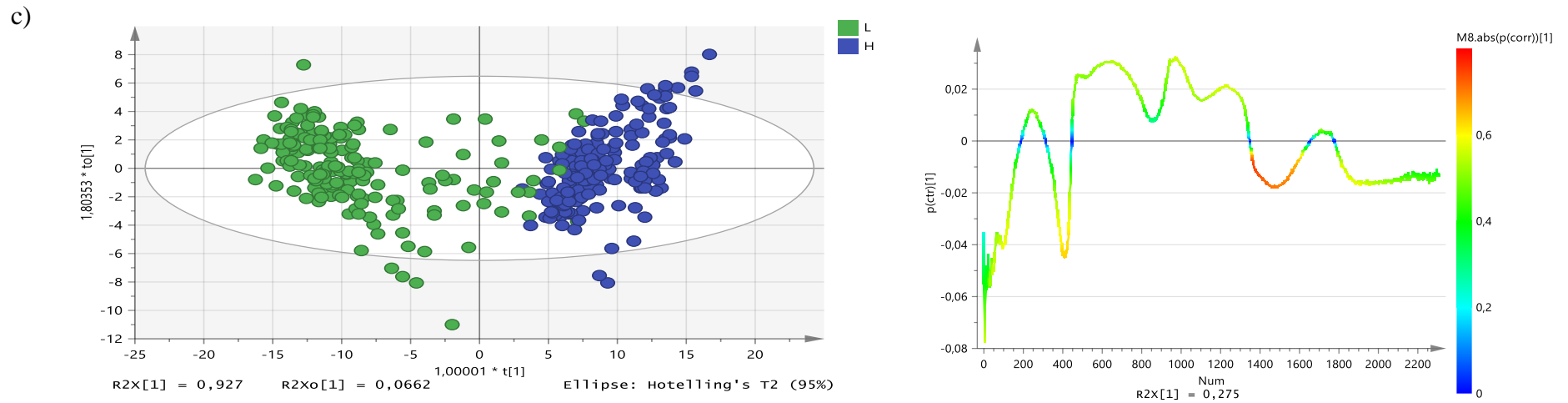


Figure 4.4 (Cont) OPLS-DA plots, for TSS (a), h^* (b), and Mass (c), with scatter score plots on the left and corresponding S-line plots on the right. TSS classes L: 4 – 8 °Brix, H: 9.1 – 15 °Brix, h^* classes L: 60 – 75 °, H: 75.1 – 120 °, Mass classes L:23-60, H: 90-162

4.3.4 Additional analysis

Fraser et al. (2003) studied the distribution of light inside mandarin fruit during internal quality assessment by NIR spectroscopy. The results in their study showed that there is rapid reduction in light level across skin of mandarin fruit and less rapid as it continues into the endocarp. This indicated that the peel region of mandarin fruit attenuates more radiation compared to the endocarp. Wang et al. (2014) showed the differences in spectra of peel and spectra of unpeeled fruit, which led to a conclusion that most information included in the spectra was from peel. The effect of peel on prediction models of ‘Satsuma’ mandarin was then investigated.

Spectra of ‘Satsuma’ mandarin while fruit was peeled was collected, at similar points as those taken on unpeeled fruit to investigate the effect of peel on NIR prediction models. Statistical indicators showed that NIR models developed using spectra of unpeeled fruit performed better than those developed using spectra of same fruit, when peeled (Supplementary Table 1). The results indicated that spectra from unpeeled fruit yielded better prediction models (with mass yielding $R^2 = 94.42$, RMSECV = 6.69g, RMSEP = 7.86 and RDP = 3.46; TSS yielding $R^2 = 73.81$, RMSEP = 1.24 Brix, RMSEP = 1.37 and RDP = 1.95, and TA R^2 yielding = 70.72, RMSECV = 0.13%, RMSEP = 0.136% and RDP = 1.64) when compared to models developed from peeled fruit (where mass yielded $R^2 = 75.77$, RMSECV = 12.6g, RMSEP = 13.2g and RPD = 1.82, TSS yielded $R^2 = 60.51$, RMSECV = 1.72, RMSEP = 2.01 and RPD = 1.34 and TA yielded $R^2 = 8.364$, RMSEP = 0.359%, RMSEP = 0.39% and RDP = 1.02).

The results indicated that the removal of peel did not improve the calibration results. Similar results were obtained by Wang et al. (2014) on ‘Navel’ orange on reflectance mode. The authors compared models developed from peeled to those developed from unpeeled spectra for ‘Navel’ oranges under interactance, reflectance and transmittance modes. Better models were achieved with unpeeled for interactance mode and reflectance, while better results were obtained with peeled spectra from transmittance mode. Wang et al. (2014) has explained that the reason for poor prediction capacity in reflectance mode with spectra from peeled fruit may be due to the major portion of orange being water making the flesh transparent, which resulted in weak diffuse reflection effect to carry enough reflective information.

Schaare & Fraser (2000) reported that calibrations in reflectance mode are susceptible to variations in surface properties of samples. Nicolai et al. (2007) on the other hand reported

that interaction of NIR with material is affected by heterogeneities such as pores, openings, which affect intensity level of reflected spectrum. The poor results obtained when fruits were peeled may therefore be attributed to the rough surface of peeled fruit.

4.4 Conclusion

The results indicated that for developing PLS prediction models, the position of fruit during scanning greatly affects prediction capacity of models. In this case the four positions along the equator gave better results than when the stem-end and stylar-end positions were included. For practical applications of NIR spectroscopy, the position of fruit during scanning must be taken into consideration. The information may be applied for on-line sorting by excluding spectra from stem-end and stylar-end of the fruit for better prediction. The results of OPLS-DA indicated that the models can separate between low values and high values for both TSS and h^* . Peeling of fruit for prediction models development did not improve prediction accuracy. Although the peel has been reported to affect penetration of light through mandarin fruit, the investigation did not reveal the effects.

References

- Abbott, J. A. (1999). Quality measurement of fruits and vegetables. *Postharvest Biology and Technology*, 15, 207–225.
- Abu-Khalaf, N., & Bennedsen, B. S. (2004). Near infrared (NIR) technology and multivariate data analysis for sensing taste attributes of apples. *International Agrophysics*, 18, 203 – 211.
- Blasco, J., Aleixos, N., & Molto. (2003). Machine vision system for automatic quality grading of fruit. *Biosystems Engineering*, 85, 415-423.
- Cayuela, J. A. (2008). Vis/NIR soluble solids prediction in intact oranges (*Citrus sinensis L.*) cv. Valencia Late by reflectance. *Postharvest Biology and Technology*, 47, 75-80.
- Cayuela, J.A., & Weiland, C. (2010). Intact orange quality prediction with two portable NIR spectrometers. *Postharvest Biology and Technology*, 58, 113 – 120.
- Department of Agriculture, Forestry and Fisheries (DAFF). (2012). Regulations relating to the grading, packing and marking of citrus fruit intended for sale in the Republic of

South Africa. http://www.gov.za/sites/www.gov.za/files/35910_9864_gon963.pdf (last accessed 29.09.2015).

Department of Agriculture, Forestry and Fisheries (DAFF). (2016). Agricultural product standards act, 1990 (Act No. 119 of 1990) standards and requirements regarding control of the export of citrus fruit. <http://www.daff.gov.za/daffweb3/Branches/Agricultural-Production-Health-Food-Safety/Food-Safety-Quality-Assurance/Export-Standards/Citrus-and-Subtropical-Fruit/Citrus-fruit> (last accessed 11.02.2017).

Eriksson, L., Byrne, T., Johansson, E., Trygg, J., & Vikstrom, C. (2006). Multi- and Megavariate data analysis, MKS Umetrics AB, Umeå, Sweden.

Fraser, D. G., Jordan, R. B., Kunnemeyer, R., & McGlone, V. A. (2003). Light distribution inside mandarin fruit during internal quality assessment by NIR spectroscopy. *Postharvest Biology and Technology*, 27, 185-196.

Gomez, A.H., He, Y., & Pereira, A.G. (2006). Non-destructive measurement of acidity, soluble solids and firmness of Satsuma mandarin using Vis-NIR spectroscopy techniques. *Journal of Food Engineering* 77, 313 - 319.

Guthrie, J. A., Walsh, K. B., Reid, D. J., & Liebenberg, C. J. (2005a). Assessment of internal quality attribute of mandarin fruit. 1. NIR calibration model development. *Australian Journal of Agricultural Research*, 56, 405-416.

Guthrie, J. A., Reid, D. J., & Wash, K. B. (2005b). Assessment of internal quality attributes of mandarin fruit. 2. NIR calibration model robustness. *Australian Journal of Agricultural Research*, 56, 417 - 426.

Jamshidi, B., Minaei, S., Mohajerani, E., & Ghassemian, H. (2012). Reflectance Vis/NIR spectroscopy for non-destructive taste characterization of Valencia oranges. *Computers and Electronics in Agriculture*, 85, 64 – 69.

Kotwaliwale, N., Singh, K., Kalne, A., Jha, S. N., Seth, N., & Kar, A. (2014). X-ray imaging methods for international quality evaluation of agricultural produce, *Journal of Food Science and Technology*, 51, 1-15.

- Liu, Y., Sun, X., Zhang, H., & Aiguo, O. (2010). Nondestructive measurement of internal quality of Nanfeng mandarin fruit by charged coupled device near infrared spectroscopy. *Computers and Electronics in Agriculture*, 71S, S10 – S14.
- Louw, E. D., & Theron, K. I. (2010). Robust prediction models for quality parameters in Japanese plums (*Prunussalicina* L.) using NIR spectroscopy, *Postharvest Biology and Technology*, 58, 176–184.
- Lurie, S. (2009). Quality parameters of fresh fruit and vegetable at harvest and shelf life. In: *Optic Monitoring of Fresh and Processed Agricultural Crops*, Taylor & Francis Group, Florida, USA.
- Magwaza, L.S., Opara, U.L., Nieuwoudt, H., & Cronje, P. (2011). Non-destructive quality assessment of ‘Valencia’ orange using FT-NIR spectroscopy. In: *Proceedings of the NIR 2011, 15th International Conference on Near-Infrared Spectroscopy*, Cape Town, South Africa, 13–20 May 2011.
- Magwaza, L.S., Opara, U.L., Nieuwoudt, H., Cronje, P.J.R., Saeys, W., & Nicolai, B. (2012a). NIR Spectroscopy Applications for Internal and External Quality Analysis of Citrus Fruit-A Review. *Food and Bioprocess Technology*, 5, 425 – 444.
- Magwaza, L. S., Opara, U. L., Terry, L. A., Landahl, S., Cronje, P. J., Nieuwoudt, H., Mouazen, A. M., Saeys, W., & Nicolai, B. M. (2012b). Prediction of ‘Nules Clementine’ mandarin susceptibility to rind breakdown disorder using Vis/NIR spectroscopy. *Postharvest Biology and Technology*, 74, 1–10.
- Magwaza, L. S., Ford, H. D., Cronje, P. J. R., Opara, U. L., Landahl, S., Tatam, R. P., & Terry, L. A. (2013). Evaluation of Fourier transform-NIR spectroscopy for integrated external and internal quality assessment of ‘Valencia’ oranges. *Journal of Food Composition and Analysis*, 31, 144–154.
- Magwaza, L. S., Landahl, S., Cronje, P. J. R., Nieuwoudt, H. H., Mouazen, A. M., Nicolai, B. M., Terry, L. A., & Opara, U. L. (2014a). The use of Vis/NIRS and chemometric analysis to predict fruit defects and postharvest behaviour of ‘Nules Clementine’ mandarin fruit. *Fruit Chemistry*, 163, 267 – 274.
- Magwaza, L. S., Opara, U. L., Cronje, P. J. R., Landahl, S., Nieuwoudt, H. H., Mouazen, A. M., Nicolai, B. M., & Terry, L. A. (2014b). Assessment of rind quality of ‘Nules

- Clementine' mandarin during postharvest storage: 1. Vis/NIRS PCA models and relationship with canopy position. *Scientia Horticulturae*, 165, 410 – 420.
- Magwaza, L. S., Opara, U. L., Cronje, P. J. R., Landahl, S., Nieuwoudt, H. H., Mouazen, A. M., Nicolai, B. M., & Terry, L. A. (2014c). Assessment of rind quality of 'Nules Clementine' mandarin fruit during postharvest storage: 2. Robust Vis/NIRS PLS models for prediction of physico-chemical attributes. *Scientia Horticulturae*, 165, 421 – 432.
- Magwaza, L. S., & Opara U. L. (2015). Analytical methods for determination of sugars and sweetness of horticultural products – A review. *Scientia Horticulturae*, 184, 179-192.
- McGlone, A. V., Fraser, D. G., Jordan, R. B., & Kunemeyer, R. (2003). Internal quality assessment of mandarin fruit by vis/NIR spectroscopy. *Journal of Near Infrared spectroscopy*, 11, 323-332.
- Miller, J. N., & Miller, J. C. (2010). *Statistics and Chemometrics for Analytical Chemistry*. Pearson Education Limited, England, UK.
- Nicolai, B. M., Beullens, K., Bobelyn, E., Peirs, A., Saeys, W., Theron, K. I., & Lammertyn, J. (2007). Nondestructive measurement of fruit and vegetable quality by means of NIR spectroscopy: A review. *Postharvest Biology and Technology*, 46, 99-118.
- Nicolai, B., Defraeye, T., De Ketelaere, B., Herremans, E., Hertog, M. L. A. T. M., Saeys, W., Torricelli, A., Vandendriessche, T., & Verboven, P. (2014). Non-destructive measurement of fruit and vegetable quality. *Annual Review Food Science Technology*, 5, 285 – 312.
- Phathare, P. B., Opara, U. L., & Al-Said, F. A. (2013). Colour Measurement and Analysis in Fresh and Processed Foods: A Review. *Food Bioprocess Technology*, 6, 36-60.
- Saeys, W., Mouazen, A.M., & Ramon, H. (2005). Potential onsite and online analysis of pig manure using visible and near infrared reflectance spectroscopy. *Biosystems Engineering*, 91, 393–402.
- Sanchez, M. T., De la Haba, M. J. & Perez-Marin, D. (2013). Internal and external quality assessment of mandarins on-tree and at harvest using a portable NIR spectrophotometer. *Computers and Electronics in Agriculture*, 92, 66-74.

- Schaare, P., & Fraser, D. (2000). Comparison of reflectance, interactance and transmission modes of visible-near infrared spectroscopy for measuring internal properties of kiwifruit (*Actinidiachinensis*). *Postharvest Biology and Technology*, 20, 175–184.
- Walsh, K. B. (2005). Commercial adoption of technologies for fruit grading, with emphasis on NIRS. *Information and Technology for Sustainable Fruit and Vegetable Production*, 5, 399 – 404.
- Wang, A., Hu, D., & Xie, L. (2014). Comparison of detection modes in terms of the necessity of visible region (VIS) and influence of the peel on soluble solid content (SSC) determination of navel orange using VIS-SWNIR spectroscopy. *Journal of Food Engineering*, 126, 126-132.
- Wang, A., & Xie, L. (2014). Technology using near infrared spectroscopic and multivariate analysis to determine the soluble solids content of citrus fruit. *Journal of Food Engineering*, 143, 17-24.
- Wiklund, S., Johansson, E., Sjostrom, L., Mellerowicz, E. J., Edlund, U., Shockcor, J. P., Gottfries, J., Moritz, T., & Trygg, J. (2008). Visualization of GC/TOF-MS-Based Metabolomics data for identification of biochemically interesting compounds using OPLS class models. *Analytical Chemistry*, 80, 115 – 122.
- William, P. C., & Sobering, D. D. (1996). How do we do it: a brief summary of the methods we use in developing near infrared calibrations. In A. M. C Davies, P Williams (Eds), *Near Infrared Spectroscopy: the future waves*. Proceedings of the 7th international Conference of Near Infrared Spectroscopy (pp. 185 – 188). Montreal, UK.
- Xudong, S., Hailiang, Z. & Yande, L. (2009). Nondestructive assessment of quality of Nafeng mandarin fruit by a portable near infrared spectroscopy. *International Journal of Agricultural and Biological Engineering*, 2, 1, 65 – 71.
- Zude, M., Pflanz, M., Kaprielian, C., & Aivazian, B. L. (2008). NIRS as a tool for precision horticulture in citrus industry. *Biosystems Engineering*, 99, 455 - 459.

5. General conclusions

5.1 Detection of granulation in ‘Navel’ orange and ‘Nadorcott’ mandarin seeds using X-ray computed tomography

X-ray CT was used to detect presence of granulation in ‘Navel’ orange and seeds in ‘Nadorcott’ mandarin. Although the technique has been applied to detect granulation in ‘Navel’ orange, detection and quantification based on tomographic images has not been investigated. This study investigated detection of granulation and quantification based on both tomographic and radiographic images. Detection of seeds in ‘Nadorcott’ mandarin was also investigated. X-ray CT has shown the ability to reveal granulation based on both radiographic and tomographic images. Accurate classifications were achieved when using radiographic and when tomographic images. The results showed the ability of X-ray CT for classification of fruit according to granulation and non-granulation. In contrary to granulation detection, seeds detection was not possible with radiographic images. Although seeds were observed on tomographic images, possible classification could not be explored due to similarities in pixel intensities between seeds and fruit flesh. To be able to detect and classify citrus based on presence of seeds, the sensitivity of the technique may be enhanced to increase image resolution and image contrast. Considering commercial application of this technique on packing lines, the technique can be applied using either the tomographic images or radiographic images as they both gave accurate classification results. While tomographic images gave slightly superior results, it may slightly time consuming as reconstruction of images from radiographic images may take a while unless methods for improving the reconstruction process are applied.

5.2 Classification of ‘Satsuma’ mandarin fruit based on physicochemical quality attributes using near infrared spectroscopy

The study aimed to investigate influence of the position of fruit during scanning on near infrared (NIR) spectroscopy model prediction accuracy and to classify ‘Satsuma’ mandarin fruit based on physicochemical attributes predicted. NIR spectroscopy has shown the ability to detect mass, sugar content (TSS), and colour (h^*) in ‘Satsuma’ mandarin fruit. The accurate classification of fruit based on the physical quality content demonstrated that the NIR spectroscopy technique can be applied in packing line for classification of fruits.

However, the manner in which fruit is placed during scanning for prediction of quality parameters has shown to have an influence on prediction models accuracies and will therefore have to be taken into account. The four positions along the equator gave better results than when the stem-end and stylar-end positions were included. Including the stylar-end and stem-end has demonstrated to compromise the data and this may be due to the two positions not containing much information about the internal quality. For investigation of the effect of peel, removal of the peel during models development did not show any improvement of prediction models. The poor results obtained when fruits were peeled were attributed to the rough surface of peeled fruit as NIR absorption is affected by heterogeneities. NIR spectroscopy has also shown the ability to classify fruit according to high and low values of mass, TSS and h^* . The technique has shown ability to detect physicochemical quality content and classification of the fruit.

The work makes a significant contribution to the potential detection of granulation, prediction physicochemical content in citrus, and classification of citrus based on the quality parameters using X-ray CT and NIR spectroscopy techniques. A combination of NIR spectroscopy and X-ray CT can enable development of multi evaluation systems in the packing lines for non-destructive evaluation of citrus. These non-destructive technologies have shown a great potential for quality evaluation and classification of fruit based on physicochemical quality parameters as well as granulation.

Supplementary Table 1 Model evaluation statistics for unpeeled and peeled spectra; calibration (R^2 , RMSECV) and validation (RMSEP and RPD) as determined from NIR spectra and reference physicochemical measurements

Parameter			Calibration			Validation			Pre-processing	Wavelength (nm)
			R^2	RMSECV	Slope	R	RMSEP	RPD		
4 positions, Peeled	scan	mass (g)	75.77	12.6	0.641	69.82	13.2	1.82	COE	7502.1-5446.3
		TSS ($^{\circ}$ Brix)	60.51	1.72	-0.105	43.67	2.01	1.34	COE	18451-7498.3,6102-5774.1
		TA (%)	8.364	0.359	0.00224	4.339	0.397	1.02	MMN	9403.7-7498.3,6102-5446.3,4601.6-4246.7
4 positions, unpeeled	scan	Mass (g)	94.42	6.69	-0.198	91.16	7.86	3.46	COE	9403.7-4597.7
		TSS ($^{\circ}$ Brix)	73.81	1.24	-0.125	73.76	1.37	1.95	MSC	9403.7-6098.1,4601.6-4246.7
		TA (%)	70.72	0.13	-0.002	62.99	0.136	1.64	MMN	9403.7-7498.3,4601.6-4246.7

R^2 : Coefficient of determination, RMSECV: root mean square error of cross validation (same units as quality parameter), RMSEP: root mean square error of prediction (same units as quality parameter), RPD: ratio of prediction to deviation, MSC: Multiplicative scattering correction, SLS: Straight line correlation, SNV: Vector normalization, TSS: Total soluble solids, TA: Titratable acidity.